Since January 2020 Elsevier has created a COVID-19 resource centre with free information in English and Mandarin on the novel coronavirus COVID-19. The COVID-19 resource centre is hosted on Elsevier Connect, the company's public news and information website.

Computers in Biology and Medicine 124 (2020) 103967

Contents lists available at ScienceDirect

Computers in Biology and Medicine

journal homepage: http://www.elsevier.com/locate/compbiomed

Immunoinformatics-guided design of an epitope-based vaccine against severe acute respiratory syndrome coronavirus 2 spike glycoprotein

Ahmed Rakib [a], Saad Ahmed Sami [a], Nusrat Jahan Mimi [a], Md. Mustafiz Chowdhury [a], Taslima Akter Eva [a], Firzan Nainu [b], Arkajyoti Paul [c,d], Asif Shahriar [e], Abu Montakim Tareq [f], Nazim Uddin Emon [f], Sajal Chakraborty [d], Sagar Shil [d], Sabrina Jahan Mily [g], Taibi Ben Hadda [h,i,*], Faisal A. Almalki [i], Talha Bin Emran [d,**]

[a] Department of Pharmacy, Faculty of Biological Sciences, University of Chittagong, Chittagong, 4331, Bangladesh
[b] Faculty of Pharmacy, Hasanuddin University, Tamalanrea, Kota Makassar, Sulawesi Selatan, 90245, Indonesia
[c] Drug Discovery, GUSTO A Research Group, Chittagong, 4203, Bangladesh
[d] Department of Pharmacy, BGC Trust University Bangladesh, Chittagong, 4381, Bangladesh
[e] Department of Microbiology, Stamford University Bangladesh, 51 Siddeswari Road, Dhaka, 1217, Bangladesh
[f] Department of Pharmacy, International Islamic University Chittagong, Chittagong, 4318, Bangladesh
[g] Department of Gynaecology and Obstetrics, Banshkhali Upazila Health Complex, Jaldi Union, Chittagong, 4390, Bangladesh
[h] Laboratory of Applied Chemistry & Environment, Faculty of Sciences, University Mohammed the First, BP 524, 60000, Oujda, Morocco
[i] Department of Pharmaceutical Chemistry, Faculty of Pharmacy, Umm Al-Qura University, Makkah Almukkarramah, 21955, Saudi Arabia

ARTICLE INFO

Keywords:
COVID-19
SARS-CoV-2
Spike glycoprotein
Immunoinformatics
Epitope

ABSTRACT

Aims: With a large number of fatalities, coronavirus disease-2019 (COVID-19) has greatly affected human health worldwide. Severe acute respiratory syndrome coronavirus 2 (SARS-CoV-2) is the virus that causes COVID-19. The World Health Organization has declared a global pandemic of this contagious disease. Researchers across the world are collaborating in a quest for remedies to combat this deadly virus. It has recently been demonstrated that the spike glycoprotein (SGP) of SARS-CoV-2 is the mediator by which the virus enters host cells.

Main methods: Our group comprehensibly analyzed the SGP of SARS-CoV-2 through multiple sequence analysis and a phylogenetic analysis. We predicted the strongest immunogenic epitopes of the SGP for both B cells and T cells.

Key findings: We focused on predicting peptides that would bind major histocompatibility complex class I. Two optimal epitopes were identified, WTAGAAAYY and GAAAYYVGY. They interact with the HLA-B*15:01 allele, which was further validated by molecular docking simulation. This study also found that the selected epitopes are able to be recognized in a large percentage of the world's population. Furthermore, we predicted $CD4^+$ T-cell epitopes and B-cell epitopes.

Significance: Our study provides a strong basis for designing vaccine candidates against SARS-CoV-2. However, laboratory work is required to validate our theoretical results, which would lay the foundation for the appropriate vaccine manufacturing and testing processes.

1. Introduction

Pandemics caused by severe life-threatening human pathogens have played a significant role in shaping human history. The world is currently battling a global pandemic rapidly developed in late December 2019. A cluster of pneumonia cases of unknown etiology was reported in Wuhan, the capital city of the Hubei Province in the People's Republic of China. Later, it was revealed that the causative agent of this outbreak was a novel coronavirus named SARS-CoV-2 (previously named 2019-nCoV). The clinical condition associated with this novel coronavirus is referred to as COVID-19 [1–3]. On March 11, 2020 the World Health Organization (WHO) categorized the current outbreak of COVID-19 as a

* Corresponding author. Laboratory of Applied Chemistry & Environment, Faculty of Sciences, University Mohammed the First, BP 524, 60000, Oujda, Morocco.
** Corresponding author. Department of Pharmacy, BGC Trust University Bangladesh, Chittagong-4381, Bangladesh.
E-mail addresses: taibi.ben.hadda@gmail.com (T. Ben Hadda), talhabmb@bgctub.ac.bd (T.B. Emran).

https://doi.org/10.1016/j.compbiomed.2020.103967
Received 28 May 2020; Received in revised form 8 August 2020; Accepted 8 August 2020
Available online 13 August 2020

pandemic. This viral infection appears to constitute a major global threat to humans and has had devastating effects worldwide. As of August 3, 2020, more than 17.9 million cases and over 685,000 deaths have been reported globally. Developed countries such as the USA, Italy, Spain, France, Germany, and the United Kingdom have experienced high mortality rates [4]. The number of COVID-19 cases has continued to escalate exponentially and is considered to be the largest outbreak of atypical pneumonia in recent times.

Tyrell and Bynoe first described the coronaviruses in 1966 [5]. Coronaviruses are pleomorphic or spherical particles with a positive single-strand RNA (+ssRNA). These viruses are very common among mammals and birds and can be transmitted to humans through pathogen spillover. They were named "coronavirus" because these virions consist of a core-shell and 9–12 nm-long crown-like surface spikes located on the outer surface of the virus, resembling a solar corona. Their genome size is the largest among all the RNA viruses, ranging from 27 to 32 kb in length, which encodes structural and nonstructural proteins of the coronavirus. Phenotypic and genotypic diversity allows them to adapt to new environments through mutation and recombination. Mutations that impact the surface proteins enable its sustainability and are challenging for the immune system, which makes SARS-CoV-2 infection unique compared to previous coronaviruses [6]. Among the four genera of coronaviruses (alpha, beta, gamma, and delta), the betacoronaviruses can cause severe disease and death in humans [7]. Including SARS-CoV-2, seven subtypes of coronaviruses have been identified in recent decades, all of which can infect humans.

SARS-CoV-2 differs from other betacoronaviruses in terms of its significantly higher infectivity and low mortality rate. It belongs to the B lineage of the betacoronavirus in the order *Nidovirales*, family *Coronaviridae*, and subfamily *Orthocoronaviridae*. After the two previously reported coronaviruses, SARS and MERS, this is the third zoonotic coronavirus outbreak of the 21st century and is closely related to its predecessors [8,9]. As it is a zoonotic virus, there is an intermediate host by which it was transmitted to humans. Preliminary investigations have predicted that SARS-CoV-2 underwent zoonotic transfer from bats to humans [9]. Primarily, environmental specimens taken from the Huanan wet market in Wuhan were found to be positive for SARS-CoV-2, but no specific association with any animal has yet been confirmed, according to a WHO report [3].

As this contagious disease is mainly a respiratory disease, it appears to affect only the lungs in most cases. The infection is transmitted between people during close contact, which occurs via the spraying of droplets from the infected individual when they cough or sneeze [10,11]. These droplets usually fall onto surfaces, and touching the contaminated surfaces followed by touching other parts of the face (such as one's eyes, nose, or mouth) may result in spreading the infection [12,13]. The symptoms of COVID-19 range from mild or moderate fever to severe pneumonia. Time from exposure to onset of symptoms ranges from 2 to 14 days, with an average of 5 days. It appears that viral spread can take place before symptoms appear. The clinical pathology largely resembles its two predecessors, with less severe upper respiratory and gastrointestinal symptoms. The most common symptoms or combination of symptoms include fever, fatigue, dry cough, dyspnea, alveolar edema, sore throat, new loss of taste or smell, and shortness of breath [14]. Older people with medical comorbidities or multi-organ failure, such as those with hypertension, cardiovascular disease, or diabetes, are more likely to become infected and suffer worse outcomes [14]. Severe cases can lead to cardiac injury, respiratory failure, acute respiratory syndrome, hepatic injury, neurological complications, or death [15].

The structure of SARS-CoV-2 includes a polyprotein (the open reading frame 1a and 1b, Orf1ab), four major structural proteins, the S protein (spike glycoprotein; SGP), E protein (envelope), M protein (membrane), and N protein (nucleocapsid), along with five accessory proteins, Orf3a, Orf6, Orf7a, Orf8 and Orf10 [16]. This novel coronavirus also encodes an additional glycoprotein that has acetyl esterase and hemagglutination (HE) attributes, and this glycoprotein does not occur in other coronaviruses [17]. Among the structural proteins, the S protein is a multifunctional molecular machine; a recent study by Walls et al. clarified the structure, function, and immunogenicity of the S protein [18]. The SGP can attach to a specific human host receptor, ACE2, on the surface of human cells. This receptor binding process mediates the entry of viral particles into the host cells with the aid of its protease, which cleaves the spike protein into the S1 and S2 subunits [19,20]. The SGP binds to ACE2, located on the surface of host cells, through the receptor binding domain (RBD), which is part of the S1 subunit. Subsequently, the viral and host membranes are fused by the S2 subunit. The viral genome RNA is released into the cytoplasm after this membrane fusion. Hence, developing neutralizing antibodies against the RBD of SARS-CoV-2 SGP might be an ideal vaccine strategy.

The identification of B-cell and T-cell epitopes for spike glycoproteins is critical for developing an effective vaccine. Although humans normally demonstrate an antibody response against viruses, only neutralizing antibodies can completely block the entry of viruses into human cells [21]. The location of antibody binding sites on a viral protein strongly affects the body's ability to produce neutralizing antibodies [22]. It is crucial to ascertain whether SARS-CoV-2 has any potential antibody binding sites (B-cell epitopes) in the RBD region, because this is the area where the virus interacts with its known human receptor, ACE2.

Apart from neutralizing antibodies, the human body also relies on cytotoxic $CD8^+$ T cells and helper $CD4^+$ T cells to eliminate viruses from the body. The presentation of a peptide will allow a B cell to receive stimulation from a helper T cell and become a plasma cell so that it can generate antibodies. T-cell epitopes in connection with MHC proteins are presented to T cells to elicit an antiviral T-cell response. Cytotoxic T cells recognize peptides that are received from the intracellular space presented by MHC class I molecules ($CD8^+$ T-cell epitopes), while helper T cells recognize extracellular peptides presented by MHC class II molecules ($CD4^+$ T-cell epitopes). The pMHC (peptide: MHC complex) interacts with the T-cell receptor and activates the cellular immune response. The inclusion of $CD4^+$ T-cell epitopes plays a key role in vaccine design, as they provide cognate help and elicit vigorous humoral and cytotoxic $CD8^+$ T cell responses and neutralizing antibodies [23]. T-cell epitope-based vaccines have been explored in recent years, as they can target conserved regions of the virus to elicit T cell responses and provide long-term protection against different strains of viruses [24].

Currently, no clinically proven vaccine grants immunity to SARS-CoV-2 infection. Researchers have examined different repurposed compounds from other viral infections to treat COVID-19, but the treatment benefit derived has been marginal or nonexistent in most cases [25]. However, with the rapid expansion of research in this area, it is hoped that a vaccine against SARS-CoV-2 could be developed in the not too distant future. To this end, several antibody development platforms have been explored, including DNA vaccines, RNA vaccines, protein subunit vaccines, virus-like particle (VLP)-based vaccines, and vector-based vaccines. However, further investigations are critical for developing a safe vaccine that is applicable in different age groups. For this purpose, extensive relevant research of the genomic and structural organization of SARS-CoV-2 is crucial. Recent studies have already reported the development of inactivated vaccine candidates against SARS-CoV-2; however, these candidates require further validation [26,27]. In addition, several institutes have isolated the SARS-CoV-2 strain for developing live-attenuated vaccine candidates; however, this type of vaccine requires extensive screening showing extremely low or no pathogenicity [28].

Many researchers have concentrated on making mRNA and DNA vaccines that eliminate the risk of any unwanted reactions. But these novel methods face many obstacles because of their experimental status and because they inherently carry very little antigenicity. Epitope-based vaccines offer a viable alternative since they can elicit potent immune responses without causing undesirable allergic reactions and have already been successfully implemented in combating other harmful

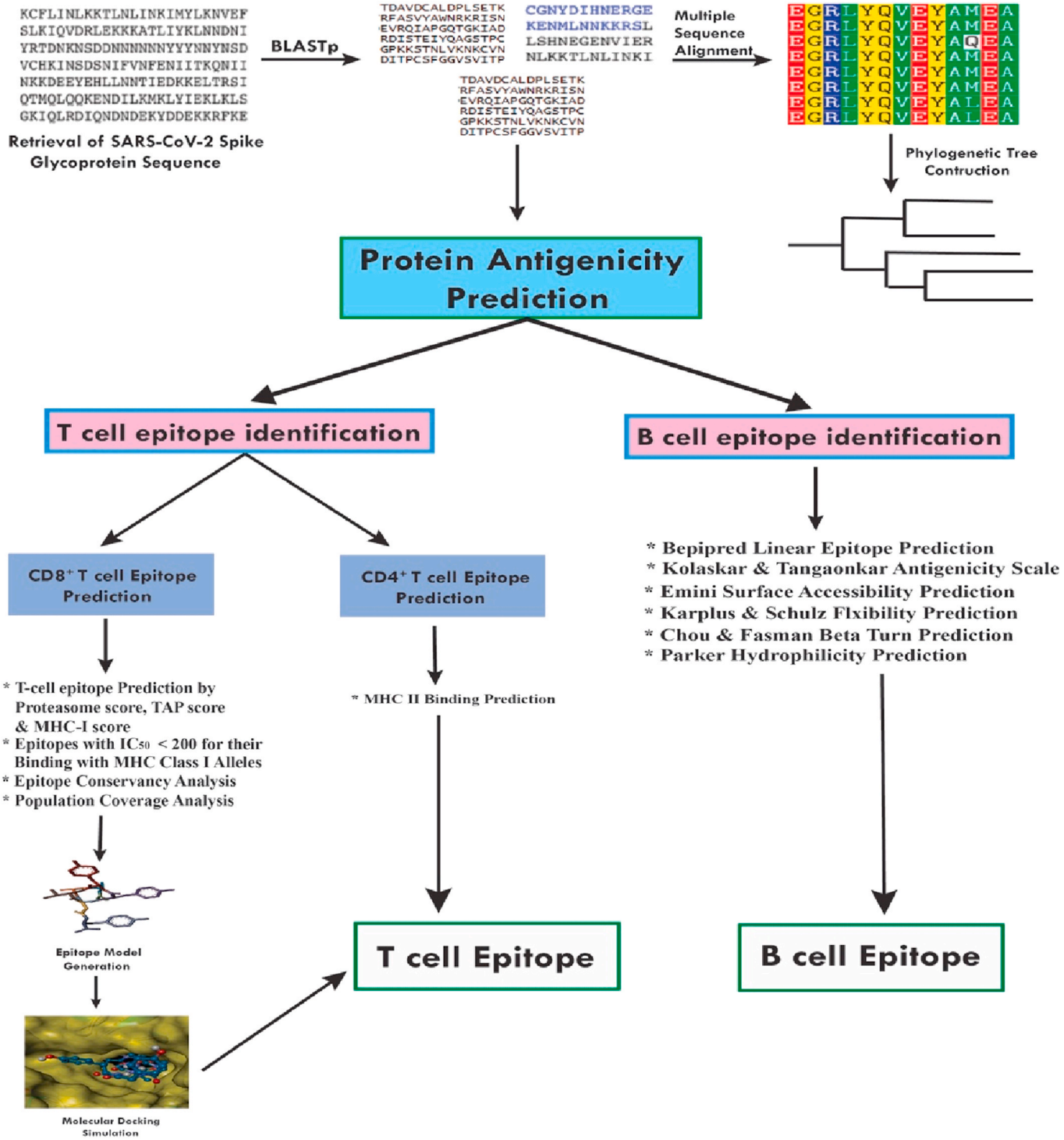

Fig. 1. Workflow of the methodologies used in epitope-based vaccine design from SARS-CoV-2 Spike Glycoprotein.

pathogens. Designing vaccines using conventional methods is not only time consuming, it is also inefficient. Various immunoinformatics tools can help to significantly speed up this laborious process. Immunoinformatics tools, such as epitope prediction, can be used to construct vaccines *in silico*, and the results can then be experimentally validated [29]. Several *in silico* immunoinformatics-guided attributes have already been predicted as a basis for an epitope-based SARS-CoV-2 vaccine; these predicted epitopes have arisen from several of the pathogen's proteins, including the N and E proteins and the main protease (M^{pro}) [30–33].

Effective promiscuous epitopes binding to a variety of human leukocyte antigen (HLA) alleles for wider dissemination with no human cross-reactivity are crucial because COVID-19 has affected populations worldwide. Our present study embarked upon the clear objective of designing an epitope-based peptide vaccine against SARS-CoV-2 infection using *in silico* methods by investigating its SGP. We targeted the epitopes of the SGP because they reportedly induce a longer-lasting immune response against SARS coronavirus [34]. We assessed the associated MHC alleles for the identified epitopes to determine those epitopes that would maximize population coverage across the world. As

Table 1
The potential $CD8^+$ T-cell epitopes along with their interacting MHC class I alleles and total processing score, epitopes conservancy hits and pMHC-I immunogenicity score.

Epitopes	NetCTL Combined score	Epitope_ Conservancy_Hit (MAX. Identity %)	MCH-I interaction with an affinity of IC50 and the total score (proteasome score, TAP score, MHC-I score, processing score)	pMHC-I immunogenicity score
WTAGAAAYY	3.1128	100	HLA-A*29:02 (1.51), HLA-A*26:01 (1.43), HLA-A*68:01 (1.12), HLA-C*12:03 (0.99), HLA-B*15:25 (0.97), HLA-B*35:01 (0.96), HLA-C*03:02 (0.91), HLA-A*30:02 (0.90), HLA-A*01:01 (0.89), HLA-B*15:01 (0.78), HLA-B*15:02 (0.68), HLA-C*16:01 (0.62), HLA-A*25:01 (0.56), HLA-C*02:09 (0.53), HLA-C*02:02 (0.53), HLA-C*12:02 (0.52), HLA-C*14:02 (0.24)	0.15259
CNDPFLGVY	1.3355	100	HLA-A*01:01 (0.36)	0.15232
GAAAYYVGY	1.2194	100	HLA-B*15:25 (1.03), HLA-A*29:02 (0.81), HLA-B*15:01 (0.69), HLA-A*30:02 (0.56), HLA-B*15:02 (0.39)	0.09963
ITDAVDCAL	1.1680	100	HLA-C*05:01 (0.62), HLA-C*08:02 (0.13), HLA-C*08:01 (0.08), HLA-C*03:04 (−0.41), HLA-C*03:03 (−0.41), HLA-C*16:01 (−0.43)	0.08501
STQDLFLPF	1.0468	100	HLA-B*15:25 (0.77), HLA-B*15:01 (0.60), HLA-B*15:02 (0.50), HLA-A*32:01 (0.48), HLA-C*16:01 (0.42), HLA-C*03:02 (0.35), HLA-B*35:01 (0.02), HLA-C*12:03 (−0.03), HLA-A*29:02 (−0.11)	0.06828
TSNQVAVLY	3.0758	100	HLA-A*01:01 (0.76), HLA-A*29:02 (0.68), HLA-A*30:02 (0.54), HLA-B*58:01 (0.33)	−0.01327
KTSVDCTMY	2.3795	100	HLA-A*30:02 (1.04), HLA-B*58:01 (0.47)	−0.11115
MTSCCSCLK	1.0963	100	HLA-A*68:01 (0.26), HLA-A*11:01 (−0.07), HLA-A*03:01 (−0.74), HLA-A*30:01 (−0.92), HLA-A*31:01 (−0.93), HLA-A*33:03 (−1.19)	−0.36816
STECSNLLL	2.3492	100	HLA-C*05:01 (−0.27)	−0.20478
GAEHVNNSY	1.9960	100	–	−0.00296

Notes: MHC-I alleles that have an interacting affinity lower than 200 nm are represented, and total processing scores are shown as enclosed numbers.

a result, using different computational tools, we designed an epitope-based peptide vaccine that would theoretically target the SARS-CoV-2 SGP with the expectation of subsequent wet laboratory validation.

2. Materials and methods

The methodologies used for peptide vaccine development for SARS-CoV-2 SGP are shown in Fig. 1.

2.1. Protein sequence retrieval and sequence analysis

The SARS-CoV-2 SGP sequence was extracted from the UniProt database (UniProt entry: P0DTC2) in FASTA format [35]. The features, function, structure, and evaluation of the sequence were mainly based on the process of sequence analysis, which subjects DNA, RNA, or peptide sequences to a wide range of analytical methods. We screened homologous sequences from the BLASTp database and selected those sequences that were most similar to that of SARS-CoV-2 SGP. We also performed multiple sequence alignment (MSA) using the ClustalW web server with default settings, and a phylogenetic tree was established using the Clustal tree format and the EMBL-EBI web server [36].

2.2. Protein antigenicity prediction

To determine the potent antigenic protein of the SARS-CoV-2 SGP, we used the online server VaxiJen v2.0, with a default threshold value [37]. All the antigenic proteins of SARS-CoV-2 SGP with their respective scores were obtained and then sorted in Notepad++.

2.3. T-cell epitope prediction

2.3.1. $CD8^+$ T-cell epitope identification

The NetCTL 1.2 server was used to identify T-cell epitopes; a 0.95 threshold was applied to maintain a sensitivity and specificity of 0.90 and 0.95, respectively [38]. The tool expanded the prediction for 12 MHC-I supertypes and unified the prediction of peptide MHC-I binding, proteasomal C-terminal cleavage with TAP transport efficiency. These predictions were performed by an artificial neural network. A weighted TAP transport efficiency matrix and a combined algorithm for MHC-I binding and proteasomal cleavage efficiency were then used to determine the overall scores and translated into sensitivity/specificity. Based on this overall score, the ten best peptides (epitopes) were selected for further evaluation.

To predict peptides that bind to MHC-I, we used a tool from the Immune Epitope Database (IEDB) to calculate half-maximal inhibitory concentration (IC_{50}) values for peptides binding to specific MHC-I molecules. For the binding analysis, all the frequently used alleles (http://tools.iedb.org/mhci/) with a word length of nine residues and a binding affinity < 200 nm were selected for further analysis [39]. The MHC-NP tool provided by the IEDB server was used to assess the probability that a given peptide was naturally processed and would bind to a given MHC molecule [40].

2.3.2. Epitope conservancy and immunogenicity prediction

The degree of similarity between the epitope and the target (i.e. given) sequence is elucidated by epitope conservancy. This property of an epitope indicates its availability in a range of different strains. The web-based tool from IEDB analysis resources was used to analyze the epitope conservancy [41]. Immunogenicity prediction can infer the degree to which a particular epitope will produce an immunogenic response. The T-cell class I pMHC immunogenicity predictor at IEDB, which uses amino acid properties as well as considering their position within the peptide, will predict the immunogenicity of a class I peptide MHC (pMHC) complex [42].

2.3.3. Allergenicity assessment

Allergenicity of the predicted epitope was calculated using AllerTop v2.0. This is an alignment-free server used for *in silico*-based allergenicity prediction of a protein based on its physicochemical properties [43].

2.3.4. Analysis of HLA–epitope interaction by molecular docking

2.3.4.1. Epitope model generation. A web-based server, PEP-FOLD, was used to predict the 3D structures of the selected epitopes [44]. For each sequence, the server predicted five probable structures. The energy of each structure was determined by SWISS-PDB VIEWER, and the structure with the lowest energy was chosen for further analysis [45].

2.3.4.2. Retrieval of HLA allele molecule. The 3D structure of the HLA-B*15:01 (PDB ID: 5TXS) was retrieved from the Protein Data Bank (RCSB-PDB) (https://www.rcsb.org/).

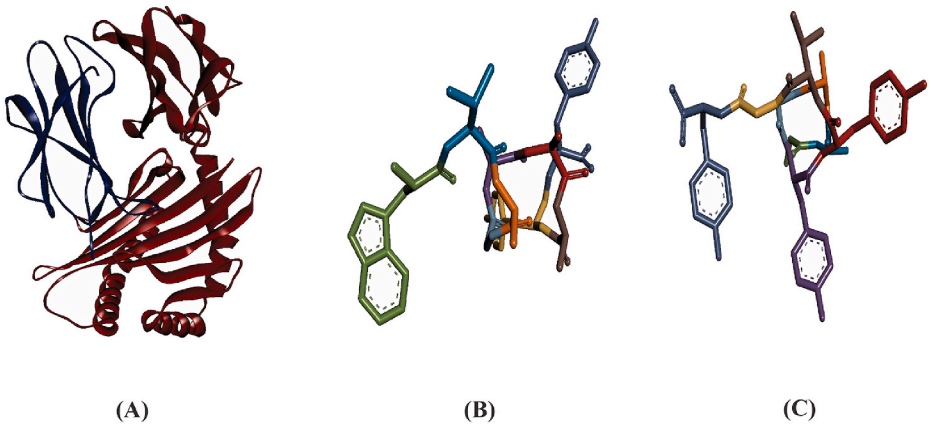

Fig. 2. Three dimensional representation of **(A)** HLA-B*15:01 allele, **(B)** Epitope WTAGAAAYY, and **(C)** Epitope GAAAYYVGY.

2.3.4.3. Molecular docking analysis. Molecular docking analysis was performed using AutoDock Vina in PyRx 0.8. The HLA-B*15:01 allele was considered as receptor protein and the identified epitopes were considered as ligand molecules [46]. First, we used the protein preparation wizard of UCSF Chimera (version 1.11.2) to prepare the protein for docking analysis by deleting the attached ligand and adding hydrogens and Gasteiger–Marsili charges. The file was then converted into pdbqt format using OpenBabel [47]. The energy form of the ligand was minimized and converted to pdbqt format by OpenBabel in PyRx 0.8. The parameters used for the docking simulation were set to default. The size of the grid box in AutoDock Vina was kept at 64.1887 × 51.9339 × 62.1079 Å for X, Y, and Z-axes, respectively. AutoDock Vina was implemented via the shell script offered by AutoDock Vina developers. The docking results were presented as negative scores in kcal/mol, as the binding affinity of a ligand with its receptor is calculated as a negative value [48].

2.4. $CD4^+$ T-cell epitope identification

To predict MHC class II potential epitopes, we utilized the MHC II prediction tools from the IEDB database (http://tools.iedb.org/mhcii/) [49]. For MHC II binding prediction, we used the human MHC alleles from Greenbaum et al. [50]. The MHC class II groove can bind peptides of different lengths. All epitopes that were predicted to bind to the alleles with an IC_{50} score of less than 50 were selected for further analysis.

2.5. Prediction of population coverage

The population coverage calculation tools from IEDB were employed to determine the individual epitope and multi-epitope population coverage for the targeted potential MHC I and MHC II alleles [51]. Here, we used the allelic frequency of the interacting HLA alleles to predict the population coverage for the corresponding epitope, both individually and combined.

2.6. Linear B-cell epitope identification

The B-cell epitope prediction aimed to identify potential antigens that would give rise to humoral immunity. To detect B-cell epitopes, various tools from IEDB were used to identify B cell antigenicity, along with Emini surface accessibility prediction, Kolaskar and Tongaonkar antigenicity scale, Karplus and Schulz flexibility prediction, and BepiPred linear epitope prediction analysis [52–55]. Because the antigenic regions of a protein are part of beta-turns, the Chou and Fasman beta-turn prediction tool was also used [56].

Table 2
Binding affinities of the selected epitopes with HLA-B*15:01.

Epitope	Binding affinity (kcal/mol)
WTAGAAAYY	−10.0
GAAAYYVGY	−9.4
STQDLFLPF	−8.3

3. Results and discussion

3.1. Sequence retrieval and analysis

The protein sequence of the SARS-CoV-2 SGP was retrieved from the UniProt database and then BLASTp was performed. From the many identified homologs, we selected only 17 that had greater than 60% sequence identity. MSA was performed **(Supplementary Data 1)** and a phylogenetic tree was constructed (Fig. S1). The MSA and phylogenetic results indicated that the protein sequences have a close relationship.

3.2. Antigenic protein prediction

The most potent antigenic protein of SARS-CoV-2 SGP was predicted by VaxiJen v2.0, which is based on the auto-cross covariance transformation of protein sequences into uniform vectors of principal amino acid properties**.** The overall antigen prediction score was 0.4683 (probable antigen) at a threshold value of 0.4. A recent review of the genomic and proteomic analysis of SARS-CoV-2 found that certain of its proteins, including M, SGP, E, and N, had the ability to confer a protective immune response against SARS-CoV-2 [57]. Additionally, a recent study proposed that epitopes on the SGP and N proteins of SARS-CoV-2 elicited strong T-cell immune responses for longer periods of time; therefore, these might be ideal vaccine candidates [58]. Significantly, the receptor-binding domain (RBD) of the SGP of two other coronaviruses, SARS-CoV and MERS-CoV, provokes strongly potent neutralizing antibody responses and have potential to be developed as vaccines against SARS and MERS infection [59,60]. In alignment with previous analyses on other coronaviruses and on other recent evidence, the current study applied computational biology techniques and immunoinformatics tools to identify an epitope-based vaccine candidate utilizing the SARS-CoV-2 SGP. We predicted the antigenicity of SGP with the VaxiJen server. However, a recent study predicted the E protein of SARS-CoV-2 to be the best immunogenic target for designing a vaccine; however, another study that used the Vaxign-ML website proposed SGP as the best vaccine candidate [32,61]. The Vaxijen tool mainly incorporates the physicochemical properties of protein sequences for its classification, but the Vaxign-ML server encompasses biological data for its predictions of vaccine candidates [62]. Several studies have documented that SGP protrudes from the virion envelope and binds to the cellular receptors, playing a crucial role in host cell entry [63,64]. Other

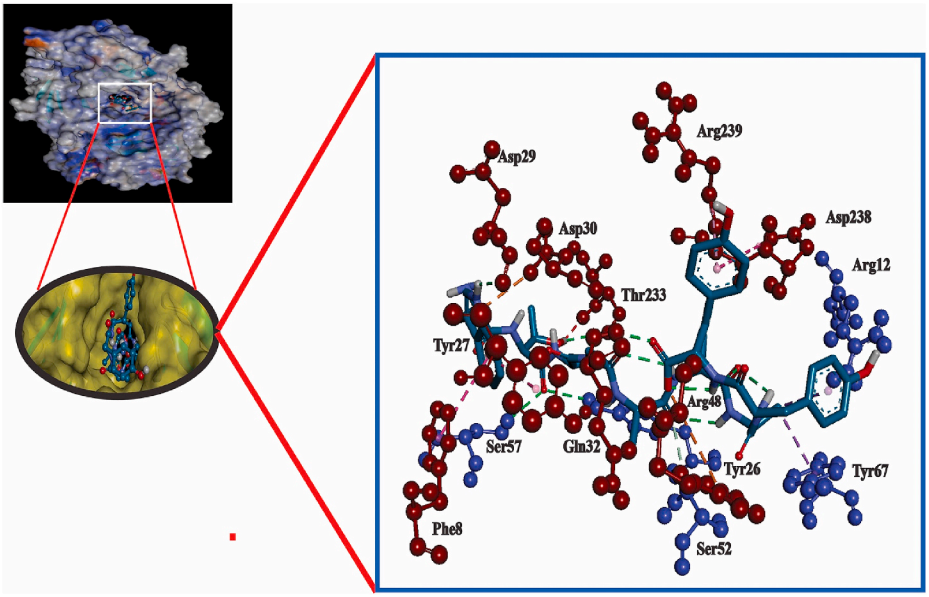

Fig. 3. Molecular docking analysis of epitope WTAGAAAYY with HLA-B*15:01 allele. The interacting A-chain residues are displayed as red ball and stick, the interacting B-chain residues are displayed in blue ball and sick, conventional hydrogen bonds are displayed as green line, pi-pi/pi-alkyl stacking are displayed as pink lines, unfavorable bumps are displayed as red lines.

research has suggested that proteins involved in viral fusion, which depends on the envelope protein and glycoprotein region, elicit the most extensive immune response, along with a cytotoxic T lymphocytes (CTL) response [65,66]. In line with previous studies and considering the best immunogenicity, we selected the SGP of SARS-CoV-2 to predict an epitope-based vaccine, which may lead to further analysis of the SARS-CoV-2 vaccination strategy.

3.3. T-cell epitope identification

3.3.1. $CD8^+$ T-cell epitope identification

On the basis of the highest combinatorial score and MHC class I binding, 23 epitopes were predicted by NetCTL 1.2 from the given protein sequence. The antigenicity of each selected peptide was predicted by VaxiJen v2.0, and we found that ten epitopes were antigenic (Table S1). The MHC-I binding prediction tool from the IEDB server was used to assess affinity; this tool is based on the stabilized matrix method. We chose the MHC-I alleles for which the epitopes showed the highest affinity ($IC_{50} < 200$ nm). Proteasomes play an important role during the conversion of protein into peptide; after proteasomal cleavage, peptide–MHC molecules are transported to the cell membrane where they are presented to T helper cells. The total score of each epitope-HLA interaction was taken into consideration; a higher score implied a higher processing efficiency. The epitope WTAGAAAYY was found to interact with 17 MHC class I alleles: HLA-A*29:02, HLA-A*26:01, HLA-A*68:01, HLA-C*12:03, HLA-B*15:25, HLA-B*35:01, HLA-C*03:02, HLA-A*30:02, HLA-A*01:01, HLA-B*15:01, HLA-B*15:02, HLA-C*16:01, HLA-A*25:01, HLA-C*02:09, HLA-C*02:02, HLA-C*12:02, and HLA-C*14:02 (Table 1). In addition, two other epitopes, namely GAAAYYVGY and STQDLFLPF, interacted with MHC I alleles. The

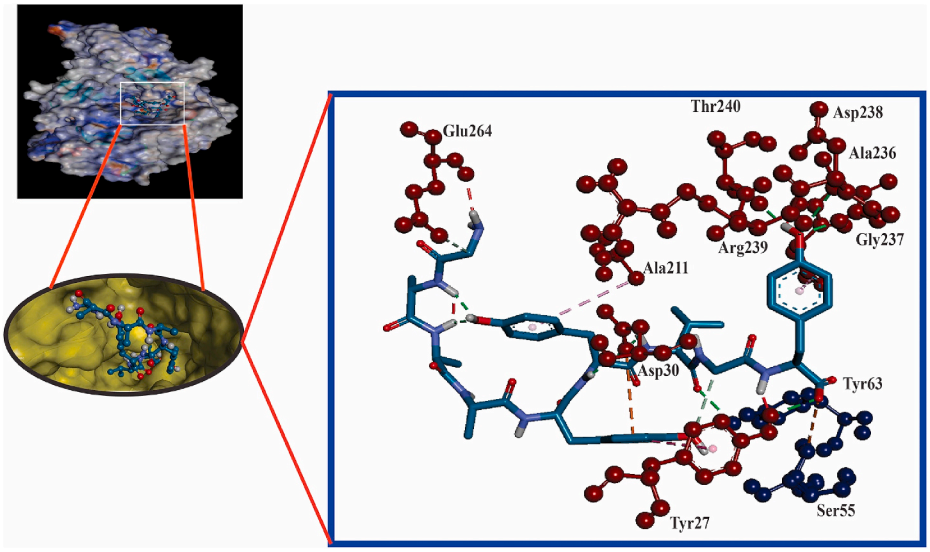

Fig. 4. Molecular docking analysis of epitope GAAAYYVGY with HLA-B*15:01 allele. The interacting A-chain residues are displayed as red ball and stick, the interacting B-chain residues are displayed in blue ball and sick, conventional hydrogen bonds are displayed as green line, pi-pi/pi-alkyl stacking are displayed as pink lines, unfavorable bumps are displayed as red lines.

Table 3
List of epitopes that had the binding affinity with the MHC Class II alleles. Notes: MHC-II alleles that have an interacting affinity lower than 50 nm are represented.

Core epitope	Allele	Percentile rank	Peptide	Start	End	SMM IC_{50}
LIVNNATNV	HLA-DRB1*13:02	0.01	KTQSLLIVNNATNVV	113	127	3.00
	HLA-DRB1*01:01	9.50	TQSLLIVNNATNVVI	114	128	49.00
IVNNATNVV	HLA-DRB1*13:02	0.01	TQSLLIVNNATNVVI	114	128	3.00
	HLA-DRB1*13:02	0.01	QSLLIVNNATNVVIK	115	129	3.00
	HLA-DRB1*13:02	0.01	SLLIVNNATNVVIKV	116	130	3.00
	HLA-DRB1*13:02	0.01	LLIVNNATNVVIKVC	117	131	4.00
	HLA-DRB1*13:02	0.03	LIVNNATNVVIKVCE	118	132	9.00
	HLA-DRB1*13:02	0.09	IVNNATNVVIKVCEF	119	133	15.00
SKTQSLLIV	HLA-DRB1*13:02	0.03	SKTQSLLIVNNATNV	112	126	8.00
QPRTFLLKY	HLA-DRB1*13:02	0.06	QPRTFLLKYNENGTI	271	285	11.00
LKYNENGTI	HLA-DRB1*13:02	0.06	PRTFLLKYNENGTIT	272	286	11.00
	HLA-DRB1*13:02	0.06	RTFLLKYNENGTITD	273	287	11.00
	HLA-DRB1*13:02	0.06	TFLLKYNENGTITDA	274	288	11.00
	HLA-DRB1*13:02	0.06	FLLKYNENGTITDAV	275	289	11.00
	HLA-DRB1*13:02	0.36	LLKYNENGTITDAVD	276	290	32.00
	HLA-DRB1*13:02	0.36	LKYNENGTITDAVDC	277	291	32.00
YNYLYRLFR	HLA-DRB1*11:01	0.09	GGNYNYLYRLFRKSN	446	460	7.00
	HLA-DRB1*11:01	0.09	GNYNYLYRLFRKSNL	447	461	7.00
	HLA-DRB1*11:01	0.29	KVGGNYNYLYRLFRK	444	458	10.00
	HLA-DRB1*11:01	0.29	VGGNYNYLYRLFRKS	445	459	10.00
FNFSQILPD	HLA-DRB1*04:05	0.21	DFGGFNFSQILPDPS	796	810	26.00
FSQILPDPS	HLA-DRB1*04:05	0.21	FGGFNFSQILPDPSK	797	811	26.00
	HLA-DRB1*04:05	0.23	GGFNFSQILPDPSKP	798	812	27.00
	HLA-DRB1*04:05	0.42	GFNFSQILPDPSKPS	799	813	38.00
	HLA-DRB1*04:05	0.42	FNFSQILPDPSKPSK	800	814	38.00
FLVLLPLVS	HLA-DRB1*01:01	0.24	MFVFLVLLPLVSSQC	1	15	5.00
	HLA-DRB1*01:01	0.24	FVFLVLLPLVSSQCV	2	16	5.00
	HLA-DRB1*04:05	0.49	MFVFLVLLPLVSSQC	1	15	41.00
	HLA-DRB1*04:05	0.52	FVFLVLLPLVSSQCV	2	16	43.00
	HLA-DRB1*11:01	0.59	MFVFLVLLPLVSSQC	1	15	18.00
	HLA-DRB1*11:01	0.59	FVFLVLLPLVSSQCV	2	16	18.00
	HLA-DRB1*01:01	1.30	VFLVLLPLVSSQCVN	3	17	11.00
	HLA-DRB1*01:01	1.80	FLVLLPLVSSQCVNL	4	18	13.00
	HLA-DRB1*11:01	2.10	VFLVLLPLVSSQCVN	3	17	45.00
VLSFELLHA	HLA-DRB1*01:01	0.24	RVVVLSFELLHAPAT	509	523	5.00
FELLHAPAT	HLA-DRB1*01:01	0.24	VVVLSFELLHAPATV	510	524	5.00
	HLA-DRB1*01:01	0.24	VVLSFELLHAPATVC	511	525	5.00
	HLA-DRB1*01:01	0.24	VLSFELLHAPATVCG	512	526	5.00
	HLA-DRB1*01:01	0.24	LSFELLHAPATVCGP	513	527	5.00
	HLA-DRB1*01:01	2.30	SFELLHAPATVCGPK	514	528	16.00
	HLA-DRB1*01:01	2.30	FELLHAPATVCGPKK	515	529	16.00
SKVGGNYNY	HLA-DRB1*11:01	0.29	SKVGGNYNYLYRLFR	443	457	10.00
FGAISSVLN	HLA-DRB1*01:01	4.20	SSNFGAISSVLNDIL	967	981	25.00
	HLA-DRB1*01:01	4.20	SNFGAISSVLNDILS	968	982	25.00
	HLA-DRB1*01:01	4.90	LSSNFGAISSVLNDI	966	980	28.00
	HLA-DRB1*01:01	5.60	QLSSNFGAISSVLND	965	979	31.00
WTFGAGAAL	HLA-DRB1*09:01	0.33	ITSGWTFGAGAALQI	882	896	42.00
	HLA-DRB1*01:01	8.90	ITSGWTFGAGAALQI	882	896	46.00
	HLA-DRB1*01:01	9.50	TSGWTFGAGAALQIP	883	897	49.00
FGAGAALQI	HLA-DRB1*09:01	0.33	SGWTFGAGAALQIPF	884	898	42.00
	HLA-DRB1*09:01	0.34	TSGWTFGAGAALQIP	883	897	43.00
	HLA-DRB1*09:01	0.35	GWTFGAGAALQIPFA	885	899	44.00
	HLA-DRB1*09:01	0.39	WTFGAGAALQIPFAM	886	900	46.00
FLPFFSNVT	HLA-DRB1*15:01	0.33	TQDLFLPFFSNVTWF	51	65	34.00
	HLA-DRB1*15:01	0.33	QDLFLPFFSNVTWFH	52	66	34.00
	HLA-DRB1*15:01	0.37	DLFLPFFSNVTWFHA	53	67	35.00
	HLA-DRB1*15:01	0.37	STQDLFLPFFSNVTW	50	64	36.00
FTISVTTEI	HLA-DRB1*07:01	0.40	AIPTNFTISVTTEIL	713	727	13.00
	HLA-DRB1*07:01	0.40	PTNFTISVTTEILPV	715	729	13.00
	HLA-DRB1*07:01	0.40	TNFTISVTTEILPVS	716	730	13.00
	HLA-DRB1*07:01	0.47	IPTNFTISVTTEILP	714	728	14.00
	HLA-DRB1*07:01	2.50	NFTISVTTEILPVSM	717	731	38.00
	HLA-DRB1*07:01	2.60	FTISVTTEILPVSMT	718	732	39.00
YGSFCTQLN	HLA-DRB1*01:01	4.90	LLQYGSFCTQLNRAL	753	767	28.00
	HLA-DRB1*04:05	0.73	LLQYGSFCTQLNRAL	753	767	49.00
FCTQLNRAL	HLA-DRB1*01:01	3.70	GSFCTQLNRALTGIA	757	771	23.00
	HLA-DRB1*01:01	3.90	YGSFCTQLNRALTGI	756	770	24.00
	HLA-DRB1*01:01	4.40	LQYGSFCTQLNRALT	754	768	26.00
	HLA-DRB1*01:01	4.40	QYGSFCTQLNRALTG	755	769	26.00
	HLA-DRB1*01:01	8.00	SFCTQLNRALTGIAV	758	772	42.00
	HLA-DRB1*01:01	8.20	FCTQLNRALTGIAVE	759	773	43.00
LYRLFRKSN	HLA-DRB1*11:01	0.42	NYNYLYRLFRKSNLK	448	462	13.00
	HLA-DRB1*11:01	0.42	YNYLYRLFRKSNLKP	449	463	13.00
	HLA-DRB1*11:01	0.52	NYLYRLFRKSNLKPF	450	464	16.00

(*continued on next page*)

Table 3 (*continued*)

Core epitope	Allele	Percentile rank	Peptide	Start	End	SMM IC_{50}
	HLA-DRB1*11:01	2.10	LYRLFRKSNLKPFER	452	466	46.00
LFLPFFSNV	HLA-DRB1*15:01	0.46	HSTQDLFLPFFSNVT	49	63	40.00
LLALHRSYL	HLA-DRB1*15:01	0.46	TRFQTLLALHRSYLT	236	250	40.00
	HLA-DRB1*11:01	2.10	RFQTLLALHRSYLTP	237	251	44.00
	HLA-DRB1*11:01	2.10	FQTLLALHRSYLTPG	238	252	44.00
TNFTISVTT	HLA-DRB1*07:01	0.47	IAIPTNFTISVTTEI	712	726	14.00
WLGFIAGLI	HLA-DRB1*01:01	4.60	WYIWLGFIAGLIAIV	1214	1228	27.00
	HLA-DRB1*01:01	8.40	WPWYIWLGFIAGLIA	1212	1226	44.00
	HLA-DRB1*01:01	8.40	PWYIWLGFIAGLIAI	1213	1227	44.00
FNGLTGTGV	HLA-DRB1*01:01	0.56	CVNFNFNGLTGTGVL	538	552	7.00
	HLA-DRB1*01:01	0.56	VNFNFNGLTGTGVLT	539	553	7.00
	HLA-DRB1*01:01	0.56	NFNFNGLTGTGVLTE	540	554	7.00
	HLA-DRB1*01:01	0.56	FNFNGLTGTGVLTES	541	555	7.00
	HLA-DRB1*01:01	3.60	NFNGLTGTGVLTESN	542	556	22.00
	HLA-DRB1*01:01	3.60	FNGLTGTGVLTESNK	543	557	22.00
LALHRSYLT	HLA-DRB1*15:01	0.58	RFQTLLALHRSYLTP	237	251	45.00
	HLA-DRB1*15:01	0.60	FQTLLALHRSYLTPG	238	252	46.00
	HLA-DRB1*15:01	0.72	QTLLALHRSYLTPGD	239	253	49.00
	HLA-DRB1*01:01	5.80	QTLLALHRSYLTPGD	239	253	32.00
	HLA-DRB1*01:01	8.40	TLLALHRSYLTPGDS	240	254	44.00
LLQYGSFCT	HLA-DRB1*15:01	0.58	CSNLLLQYGSFCTQL	749	763	45.00
	HLA-DRB1*15:01	0.60	SNLLLQYGSFCTQLN	750	764	46.00
	HLA-DRB1*15:01	0.72	ECSNLLLQYGSFCTQ	748	762	49.00
ITRFQTLLA	HLA-DRB1*01:01	1.30	GINITRFQTLLALHR	232	246	11.00
	HLA-DRB1*11:01	1.90	GINITRFQTLLALHR	232	246	41.00
FIAGLIAIV	HLA-DRB1*01:01	2.60	YIWLGFIAGLIAIVM	1215	1229	18.00
SVYAWNRKR	HLA-DRB1*11:01	0.63	TRFASVYAWNRKRIS	345	359	19.00
YAWNRKRIS	HLA-DRB1*11:01	0.63	RFASVYAWNRKRISN	346	360	19.00
	HLA-DRB1*11:01	0.63	FASVYAWNRKRISNC	347	361	19.00
	HLA-DRB1*11:01	0.63	ASVYAWNRKRISNCV	348	362	19.00
	HLA-DRB1*11:01	0.63	SVYAWNRKRISNCVA	349	363	19.00
KCVNFNFNG	HLA-DRB1*01:01	0.67	KCVNFNFNGLTGTGV	537	551	8.00
VIGIVNNTV	HLA-DRB1*13:02	0.70	CDVVIGIVNNTVYDP	1126	1140	49.00
	HLA-DRB1*13:02	0.70	DVVIGIVNNTVYDPL	1127	1141	49.00
LLLQYGSFC	HLA-DRB1*15:01	0.72	TECSNLLLQYGSFCT	747	761	49.00
FQTLLALHR	HLA-DRB1*01:01	0.91	ITRFQTLLALHRSYL	235	249	9.00
	HLA-DRB1*01:01	0.91	TRFQTLLALHRSYLT	236	250	9.00
	HLA-DRB1*11:01	1.20	ITRFQTLLALHRSYL	235	249	27.00
	HLA-DRB1*11:01	1.20	TRFQTLLALHRSYLT	236	250	27.00
	HLA-DRB1*01:01	1.30	INITRFQTLLALHRS	233	247	11.00
	HLA-DRB1*01:01	1.30	NITRFQTLLALHRSY	234	248	11.00
	HLA-DRB1*11:01	1.80	INITRFQTLLALHRS	233	247	40.00
	HLA-DRB1*11:01	1.80	NITRFQTLLALHRSY	234	248	40.00
	HLA-DRB1*01:01	3.10	RFQTLLALHRSYLTP	237	251	20.00
	HLA-DRB1*01:01	3.10	FQTLLALHRSYLTPG	238	252	20.00
LVKQLSSNF	HLA-DRB1*01:01	8.20	QALNTLVKQLSSNFG	957	971	43.00
YRLFRKSNL	HLA-DRB1*11:01	1.20	YLYRLFRKSNLKPFE	451	465	27.00
MIAQYTSAL	HLA-DRB1*01:01	6.00	LLTDEMIAQYTSALL	864	878	33.00
DYSVLYNSA	HLA-DRB1*01:01	1.30	SNCVADYSVLYNSAS	359	373	20.00
YSVLYNSAS	HLA-DRB1*01:01	2.60	CVADYSVLYNSASFS	361	375	18.00
	HLA-DRB1*01:01	2.60	ADYSVLYNSASFSTF	363	377	18.00
	HLA-DRB1*01:01	2.90	NCVADYSVLYNSASF	360	374	19.00
	HLA-DRB1*01:01	8.00	DYSVLYNSASFSTFK	364	378	42.00
	HLA-DRB1*01:01	8.00	YSVLYNSASFSTFKC	365	379	42.00
IRASANLAA	HLA-DRB1*01:01	9.30	AEIRASANLAATKMS	1016	1030	48.00
YFKIYSKHT	HLA-DRB1*11:01	1.30	NIDGYFKIYSKHTPI	196	210	28.00
	HLA-DRB1*11:01	1.30	IDGYFKIYSKHTPIN	197	211	28.00
	HLA-DRB1*11:01	1.30	KNIDGYFKIYSKHTP	195	209	29.00
	HLA-DRB1*11:01	1.30	DGYFKIYSKHTPINL	198	212	29.00
	HLA-DRB1*01:01	7.70	NIDGYFKIYSKHTPI	196	210	41.00
	HLA-DRB1*01:01,	7.70	IDGYFKIYSKHTPIN	197	211	41.00
	HLA-DRB1*01:01	7.70	DGYFKIYSKHTPINL	198	212	41.00
	HLA-DRB1*01:01	8.40	KNIDGYFKIYSKHTP	195	209	44.00
LTVLPPLLT	HLA-DRB1*01:01	1.30	FNGLTVLPPLLTDEM	855	869	11.00
	HLA-DRB1*01:01	1.60	QKFNGLTVLPPLLTD	853	867	12.00
	HLA-DRB1*01:01	1.60	KFNGLTVLPPLLTDE	854	868	12.00
	HLA-DRB1*01:01	1.60	NGLTVLPPLLTDEMI	856	870	12.00
	HLA-DRB1*01:01	6.30	GLTVLPPLLTDEMIA	857	871	34.00
	HLA-DRB1*01:01	6.80	LTVLPPLLTDEMIAQ	858	872	37.00
IDGYFKIYS	HLA-DRB1*11:01	1.30	FKNIDGYFKIYSKHT	194	208	31.00
FKNIDGYFK	HLA-DRB1*01:01	7.70	FKNIDGYFKIYSKHT	194	208	41.00
YTSALLAGT	HLA-DRB1*01:01	7.50	MIAQYTSALLAGTIT	869	883	40.00
	HLA-DRB1*01:01	8.20	IAQYTSALLAGTITS	870	884	43.00
	HLA-DRB1*01:01	9.10	AQYTSALLAGTITSG	871	885	47.00
IAGLIAIVM	HLA-DRB1*01:01	2.50	IWLGFIAGLIAIVMV	1216	1230	17.00
	HLA-DRB1*01:01	2.50	LGFIAGLIAIVMVTI	1218	1232	17.00

(*continued on next page*)

Table 3 (*continued*)

Core epitope	Allele	Percentile rank	Peptide	Start	End	SMM IC_{50}
	HLA-DRB1*01:01	2.60	WLGFIAGLIAIVMVT	1217	1231	18.00
	HLA-DRB1*01:01	3.60	GFIAGLIAIVMVTIM	1219	1233	22.00
	HLA-DRB1*01:01	8.90	FIAGLIAIVMVTIML	1220	1234	46.00
LSSNFGAIS	HLA-DRB1*01:01	5.10	KQLSSNFGAISSVLN	964	978	29.00
VKQLSSNFG	HLA-DRB1*01:01	7.70	NTLVKQLSSNFGAIS	960	974	41.00
	HLA-DRB1*01:01	8.00	LNTLVKQLSSNFGAI	959	973	42.00
	HLA-DRB1*01:01	8.90	ALNTLVKQLSSNFGA	958	972	46.00
	HLA-DRB1*01:01	8.90	TLVKQLSSNFGAISS	961	975	46.00
DSKTQSLLI	HLA-DRB1*07:01	3.30	FGTTLDSKTQSLLIV	106	120	48.00
	HLA-DRB1*07:01	3.30	GTTLDSKTQSLLIVN	107	121	48.00
	HLA-DRB1*07:01	3.30	TTLDSKTQSLLIVNN	108	122	49.00
FAMQMAYRF	HLA-DRB1*01:01	3.60	QIPFAMQMAYRFNGI	895	909	22.00
	HLA-DRB1*01:01	3.70	IPFAMQMAYRFNGIG	896	910	23.00
	HLA-DRB1*01:01	3.90	ALQIPFAMQMAYRFN	893	907	24.00
	HLA-DRB1*01:01	3.90	LQIPFAMQMAYRFNG	894	908	24.00
IAQYTSALL	HLA-DRB1*01:01	5.80	DEMIAQYTSALLAGT	867	881	32.00
	HLA-DRB1*01:01	6.30	TDEMIAQYTSALLAG	866	880	34.00
	HLA-DRB1*01:01	6.30	EMIAQYTSALLAGTI	868	882	34.00
	HLA-DRB1*01:01	6.50	LTDEMIAQYTSALLA	865	879	35.00
YLQPRTFLL	HLA-DRB1*01:01	4.40	AYYVGYLQPRTFLLK	264	278	26.00
	HLA-DRB1*01:01	4.90	YYVGYLQPRTFLLKY	265	279	28.00
	HLA-DRB1*01:01	5.60	YVGYLQPRTFLLKYN	266	280	31.00
	HLA-DRB1*01:01	5.80	VGYLQPRTFLLKYNE	267	281	32.00
ISGINASVV	HLA-DRB1*01:01	4.40	LGDISGINASVVNIQ	1166	1180	26.00
	HLA-DRB1*01:01	4.60	DLGDISGINASVVNI	1165	1179	27.00
	HLA-DRB1*01:01	4.90	GDISGINASVVNIQK	1167	1181	28.00
	HLA-DRB1*01:01	5.10	VDLGDISGINASVVN	1164	1178	29.00
QIPFAMQMA	HLA-DRB1*01:01	5.10	AALQIPFAMQMAYRF	892	906	29.00
ITGRLQSLQ	HLA-DRB1*01:01	5.80	RLITGRLQSLQTYVT	995	1009	32.00

former interacted with five HLAs and the latter interacted with nine. However, like WTAGAAAYY, both epitopes interacted with HLA-B*15:25 and HLA-B*15:01. The epitope GAAAYYVGY showed a stronger affinity for binding HLA-B*15:25, whereas WTAGAAAYY had the strongest immunogenicity predicted by the I-pMHC immunogenicity prediction analysis, and the binding affinity of WTAGAAAYY to HLA-B*15:01 was relatively higher (Table 1). Furthermore, all the predicted epitopes had a maximum identity for conservancy, and 100% maximum identity was found (Table 1). Therefore, we selected the aforementioned three epitopes for further analysis. In addition, MHC-NP found that these epitopes would naturally bind to the MHC class I alleles (Table S2).

By concentrating on potential MHC class I peptide epitopes, we predicted not only T-cell but also B-cell epitopes. Both of these epitope types are capable of showing immune responses in several ways. Many criteria must be met when identifying a protein sequence-based epitope as a potential vaccine candidate, whereby allergenicity is regarded as one of the most important factors. We input the SARS-CoV-2 SGP sequence into the VaxiJen server and predicted the antigenicity of the protein sequence. Ten potent epitopes were predicted by the NetCTL 1.2 server, and the epitopes were further used in the progressive analysis that also showed MHC class I interaction. Subsequently, all peptides except GAEHVNNSY were shown to interact with the MHC class I alleles. WTAGAAAYY interacted with the most MHC class I alleles. Among them, the allele HLA-A*29:02 had the highest binding score (1.51). Interestingly, three of the epitopes, WTAGAAAYY, GAAAYYVGY, and STQDLFLPF, showed binding interaction with the same MHA class I allele (HLA-B*15:25), of which GAAAYYVGY had the highest affinity. Additionally, the aforementioned epitopes also interacted with HLA-B*15:01, and epitope WTAGAAAYY showed the highest affinity for it.

Table 4
Analysis of the population coverage using potential MHC I and MHC II interacted alleles for the proposed multi-epitope vaccine against SARS-CoV-2.

Population/Area	MHC I Combined			MHC II Combined		
	Coverage (%)[a]	Average hit[b]	PC90[c]	Coverage (%)[a]	Average hit[b]	PC90[c]
Central Africa	63.97	1.56	0.28	46.24	1.12	0.19
Central America	2.19	0.04	0.10	23.76	0.43	0.13
East Africa	60.78	1.40	0.25	51.00	1.51	0.20
East Asia	62.39	1.49	0.27	57.95	1.65	0.24
Europe	77.91	1.86	0.45	65.71	2.16	0.29
North Africa	72.00	1.77	0.36	57.03	1.15	0.23
North America	65.50	1.59	0.29	63.77	2.01	0.28
Northeast Asia	56.06	1.54	0.23	36.94	0.77	0.16
Oceania	35.97	0.67	0.16	43.67	0.94	0.18
South Africa	70.08	1.71	0.33	5.91	0.12	0.21
South America	46.65	0.91	0.19	26.99	0.71	0.14
South Asia	69.11	1.53	0.32	60.68	1.63	0.25
Southeast Asia	44.14	1.08	0.18	35.62	0.67	0.16
Southwest Asia	60.13	1.14	0.25	31.97	0.76	0.15
West Africa	77.98	2.17	0.45	47.72	1.25	0.19
West Indies	56.56	1.22	0.23	54.15	1.72	0.22

[a] Projected population coverage.
[b] Average number of epitope hits/HLA combinations recognized by the population.
[c] Minimum number of epitope hits/HLA combinations recognized by 90% of the population.

Table 5
List of predicted B cell epitopes from BepiPred linear epitope prediction analysis.

No.	Start	End	Peptide	Length
1	21	31	RTQLPPAYTNS	11
2	71	81	SGTNGTKRFDN	11
3	249	261	LTPGDSSSGWTAG	12
4	318	324	FRVQPTE	7
5	407	420	VRQIAPGQTGKIAD	14
6	439	447	NNLDSKVGG	9
7	473	483	YQAGSTPCNGV	11
8	495	506	YGFQPTNGVGYQ	12
9	523	532	TVCGPKKSTN	10
10	567	580	RDIADTTDAVRDPQ	14
11	597	606	VITPGTNTSN	10
12	675	687	QTQTNSPRRARSV	13
13	772	780	VEQDKNTQE	9
14	788	797	IYKTPPIKDF	10
15	805	816	ILPDPSKPSKRS	12
16	1069	1077	PAQEKNFTT	9
17	1137	1148	VYDPLQPELDSF	12
18	1157	1167	KNHTSPDVDLG	11
19	1256	1265	FDEDDSEPVL	10

In addition, the epitope conservancy was predicted by the IEDB conservancy analysis tool, and all of our predicted epitopes had a maximum identity of 100%. Hence, these three epitopes were selected for further analysis.

3.3.2. Allergenicity assessment

The AllerTop server assesses the allergic reactions caused by a vaccine candidate in an individual that might be harmful or life-threatening. The allergenicity of the selected epitopes was calculated using the AllerTop tool, and they were predicted as probable non-allergens.

Allergenicity is regarded as a notable obstacle during vaccine development. $CD4^+$ T cells are the primary actors responsible for provoking an allergic reaction, but immunoglobulin E and type 2 T helper cells can also stimulate allergic reactions [67]. We evaluated the allergenicity using AllerTop 2.0. This tool is well-known for its high sensitivity to identify new allergens in relation to known allergens [43]. AllerTop predicted our selected epitopes to be non-allergenic.

3.3.3. Molecular docking analysis of the HLA–epitope interaction

Here, the interaction between the HLA molecules and our predicted potential epitopes was validated by molecular docking simulation using AutoDock Vina in PyRx 0.8. We previously found that alleles HLA-B*15:25 and HLA-B*15:01 interacted with the three predicted epitopes. However, the 3D structure of HLA-B*15:25 was not available in the Protein Data Bank (PDB). Although the binding affinities of the selected epitopes were greater for HLA-B*15:25, we selected HLA-B*15:01 for study because it was available from the PDB database. The structures of HLA-B*15:01 and the selected epitopes are shown in Fig. 2. For the docking analysis, we considered the HLA molecule as the receptor and the selected three epitopes as ligand molecules. The docking experiments showed that the epitope WTAGAAAYY interacted with HLA-B*15:01 with the highest binding affinity, which was calculated as −10.0 kcal/mol; the binding affinity of GAAAYYVGY was almost equal to that of GAAAYYVGY (−9.4 kcal/mol) (Table 2)). By visualizing the docking r. However, the binding affinity of the epitope STQDLFLPF was found to be only −8.3 kcal/mol (Table 2). By visualizing the docking results, it was clear that WTAGAAAYY formed hydrogen bonds (H-bonds) with six amino acid residues (Gln32, Thr233, Asp29 from the A-chain; Arg12, Tyr26, Ser7 from the B-chain) and pi-pi stacking with Asp238, Tyr27, and Phe8 from the A-chain (Fig. 3). No unfavorable bonds were visualized for the epitope WTAGAAAYY, albeit two unfavorable donor-donor bonds were found for GAAAYYVGY. In addition, more H-bonds were found for GAAAYYVGY, including six from A-chain residues (Asp238, Gly237, Thr240, Arg239, Asp30, Tyr27) and one from Tyr63 in the B-chain. There were also favorable interactions with Ser55 from the B-chain, and pi-pi stacking was visualized for Tyr27 from the A-chain, which also formed a H-bond with the HLA molecule (Fig. 4).

MHC class I and class II molecules play a pivotal role by presenting peptides on the cell surface that can then be identified by T cells. MHC I class molecules present shorter molecules (generally 8–11 amino acids long), and MHC class II molecules present longer peptides (typically 13–17 amino acid residues) [68]. In the current study, we determined the binding affinity of the predicted peptide sequences with HLA-B*15:01 because the structure of this allele was available in the PDB database. The findings from the molecular docking analysis revealed that epitopes WTAGAAAYY and GAAAYYVGY had the highest affinity interactions with the HLA-B*15:01 allele, as a more negative result implies a stronger interaction [69]. Furthermore, these two epitopes were able to interact with the allele through H-bonds and hydrophobic (pi-pi stacking, pi-alkyl) interactions, and attractive charges also contributed to binding in the case of GAAAYYVGY. Conversely, the epitope STQDLFLPF had a less negative docking score; hence, its binding interaction was weaker in comparison with the other two epitopes.

3.4. Predication of T helper cell epitopes and MHC class II interaction analysis

In this experiment, potential $CD4^+$ T-cell peptide epitopes were identified by the MHC class II prediction tool from the IEDB website, which provided 56 core epitopes for the selected HLA-DRB alleles with an $IC_{50} < 50$ nm. The peptides with the core epitopes IVNNATNVV, LKYNENGTI, FLVLLPLVS, FELLHAPAT, FTISVTTEI, FCTQLNRAL, FNGLTGTGV, LALHRSYLT, FQTLLALHR, and YFKIYSKHT interacted with most of the MHC class II alleles. These results are shown in Table 3.

Vaccination strategies that only depend on $CD8^+$ T-cell immunity might be inadequate, because although $CD8^+$ T cells stimulate extremely early responses, they might be unable to elicit long-term protective responses [70]. $CD4^+$ T cells play a pivotal role in the adaptive immune response by maintaining and promoting the expansion of cytotoxic T cells, maintaining the memory of $CD8^+$ T cells, and communicating with the innate immune cells [23]. In addition, $CD4^+$ cells help $CD8^+$ cells to generate strong primary and memory responses, as well as protective immunity against many types of bacterial and viral infections [71,72]. Previously, the development of vaccines was rudimentarily based on B cell immunity, whereas more recently it has been well established that T-cell epitopes provide a more long-lasting immune response, which is primarily mediated by $CD4^+$ T cells as a result of antigenic drift [73]. The prediction of $CD4^+$ T-cell epitopes mainly focuses on the peptide binding to the MHC class II proteins [74]. In the current study, we predicted several $CD4^+$ T-cell epitopes by applying the criterion of $IC_{50} < 50$ nm. This threshold is considered to indicate more favorable immunogenic properties of the predicted T-cell epitopes, where a lower IC_{50} value represents a higher binding affinity [75]. The current research work is more specific than several previous studies, for instance, Alam et al. used $IC_{50} < 100$ nm for predicting $CD4^+$ T-cell epitopes [76]. Moreover, our predicted T-cell epitopes were identical to the epitopes predicted in previous studies. The peptides with the core epitopes LIVNNATNV, IVNNATNVV, SKTQSLLIV, YNYLYRLFR, FNFSQILPD, SKVGGNYNY, YGSFCTQLN, LYRLFRKSN, LLALHRSYL, WLGFIAGLI, LALHRSYLT, LLQYGSFCT, FIAGLIAIV, FQTLLALHR, LVKQLSSNF, YRLFRKSNL, IRASANLAA, IAGLIAIVM, and ITGRLQSLQ were identical to those found in the previous study by Grifoni et al., which mapped the T-cell epitopes of SARS-CoV and SARS-CoV-2 [77]. Further, our predicted peptide AALQIPFAMQMAYRF (region 892–906) interacts with HLA-DRB1*01:01, which is in line with the previous study by Ahmed et al. [16].

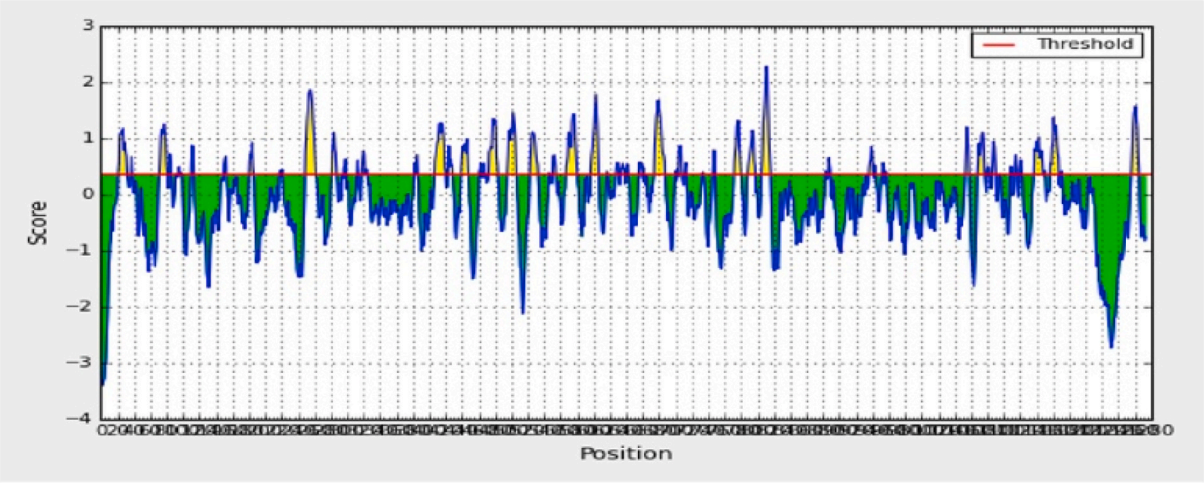

(A)

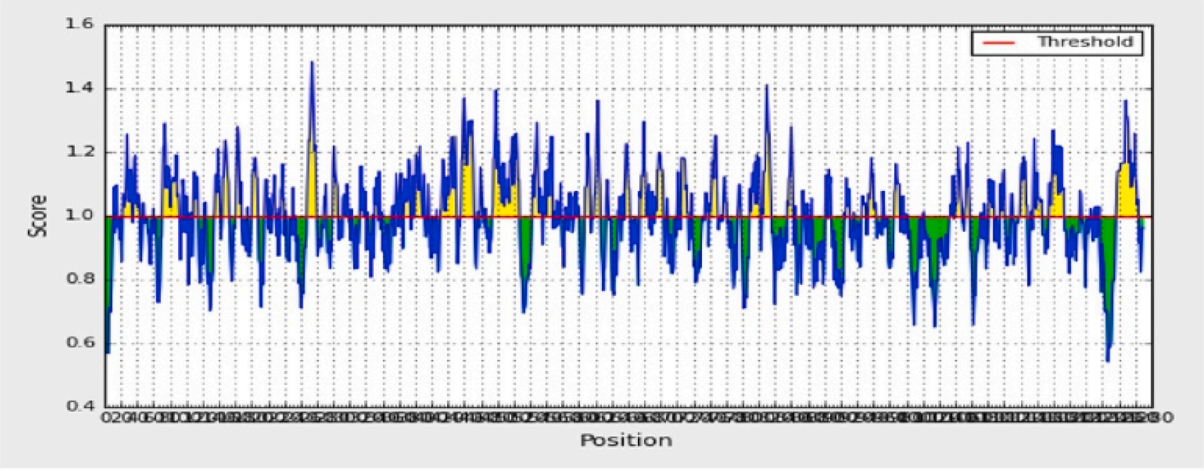

(B)

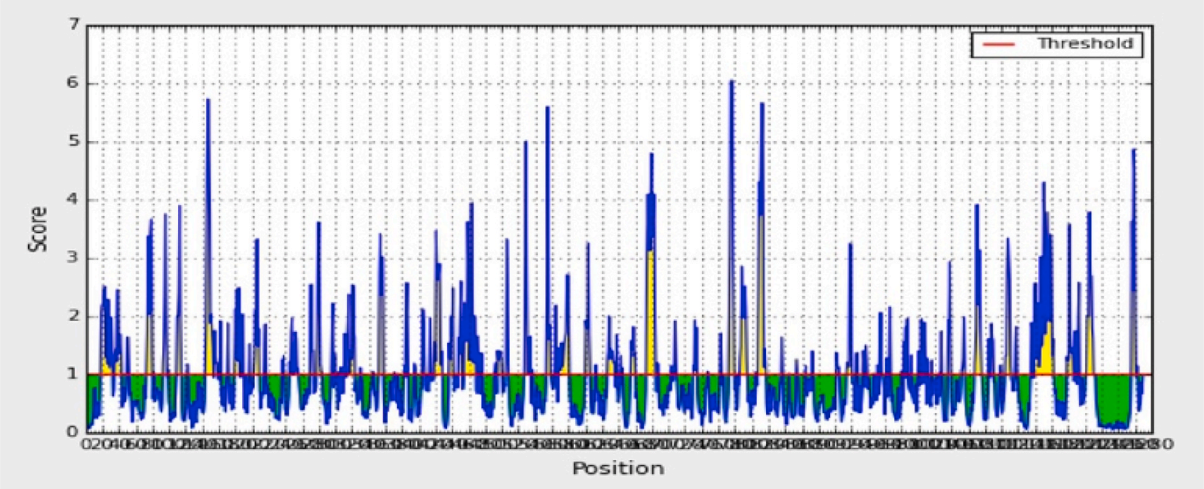

(C)

Fig. 5. Combined B-cell linear epitope prediction using **(A)** Bepipred linear epitope prediction, **(B)** Chou & Fasman beta-turn prediction, **(C)** Emini surface accessibility prediction methods.

Table 6
List of predicted B-cell epitopes from Kolaskar and Tongaonkar antigenicity prediction method.

Start	End	Peptide	Length
4	18	FLVLLPLVSSQCVNL	15
34	41	RGVYYPDK	8
44	51	RSSVLHST	8
53	60	DLFLPFFS	8
81	87	NPVLPFN	7
115	121	QSLLIVN	7
125	134	NVVIKVCEFQ	10
136	146	CNDPFLGVYYH	11
168	174	FEYVSQP	7
210	216	INLVRDL	7
223	230	LEPLVDLP	8
239	248	QTLLALHRSY	10
263	270	AAYYVGYL	8
272	278	PRTFLLK	7
288	295	AVDCALDP	8
333	339	TNLCPFG	7
359	371	SNCVADYSVLYNS	13
376	385	TFKCYGVSPT	10
488	495	CYFPLQSY	8
505	527	YQPYRVVVLSFELLHAPATVCGP	23
592	599	FGGVSVIT	8
607	615	QVAVLYQDV	9
617	627	CTEVPVAIHAD	11
647	653	AGCLIGA	7
667	674	GAGICASY	8
687	693	VASQSII	7
723	730	TTEILPVS	8
735	741	SVDCTMY	7
750	763	SNLLLQYGSFCTQL	14
781	788	VFAQVKQI	8
837	843	YGDCLGD	7
847	853	RDLICAQ	7
858	864	LTVLPPL	7
873	880	YTSALLAG	8
959	966	LNTLVKQL	8
973	979	ISSVLND	7
1003	1011	SLQTYVTQQ	9
1030	1037	SECVLGQS	8
1057	1070	PHGVVFLHVTYVPA	14
1079	1085	PAICHDG	7
1123	1132	SGNCDVVIGI	10
1174	1179	ASVVNI	12
1221	1256	IAGLIAIVMVTIMLCCMTSCCSCLKGCCSCGSCCKF	36

3.5. Population coverage analysis

We first analyzed the individual epitopes that interacted with MHC class I alleles. West Africa had the highest coverage region for epitopes WTAGAAAYY and STQDLFLPF, at 76.33% and 58.93%, respectively (Table S3). South Asia had the highest coverage region for the epitope GAAAYYVGY, at 32.67% (Table S3). Next, we performed a population coverage analysis combining multiple epitopes. The cumulative population coverage was obtained for the three predicted epitopes, WTAGAAAYY, GAAAYYVGY, and STQDLFLPF. For the population coverage analysis of the multiple epitopes, the results were in agreement with those of the individual predicted epitopes, showing 77.98% coverage for West Africa, which was the highest coverage region. Europe had the second-highest coverage, at 77.91% (Table 4). The population coverage results for MHC class I alleles are shown in Fig. S2-S5.

We next conducted a population coverage analysis for MHC class II alleles. As in the MHC class I analysis, we first individually predicted the population coverage for the MHC II alleles to find the maximum MHC II interaction. The core epitope LALHRSYLT showed the maximum coverage, which was 34.63% for the North American region (Table S4). Three core epitopes, namely YFKIYSKHT, FLVLLPLVS, and FQTLLALHR, exhibited greater than 25% coverage for Europe (Table S4). Epitope FLVLLPLVS showed 33.74% and 34.08% coverage for East Africa and East Asia, respectively (Table S4). The cumulative coverage of the targeted epitopes interacting with MHC class II alleles was then analyzed. The predicted epitopes were found to have a coverage of greater than 60% for three regions, Europe, North America, and South Asia, of which the maximum coverage was for Europe (65.71%) (Table 4).

Population coverage is important to understand during vaccine development because HLA varies by ethnicity and geographical region. We utilized the population coverage tool from IEDB to conduct the population coverage analysis for the predicted three epitopes, both individually and combined, for MHC class I and II alleles. Individually, for MHC class I alleles, West Africa had the highest percentage of population coverage for epitope WTAGAAAYY, followed by STQDLFLPF. The individual population coverage analysis for MHC class I alleles showed that the coverage for epitope WTAGAAAYY was greater than 50% for most regions, whereas GAAAYYVGY covered less than 40% of all regions. The selected three epitopes combined covered almost all available regions worldwide, and the highest coverage was observed in West Africa. Surprisingly, of the regions where the most cases of the infection were reported (namely, Europe and North America), the coverage was greater than 65%; thus, the coverage of Europe was nearly identical to that of West Africa. Interestingly, the epitopes showed 62.39% coverage in East Asia, where the first COVID-19 case was reported. The results of our predictions agree with those of Ahmed et al., who found that a multi-epitope vaccine has a larger population coverage [16]. However, like a multi-epitope vaccine, WTAGAAAYY individually covered most of the world's population. In addition, the predicted epitopes that interacted with the MHC class II alleles showed results similar to those of the MHC class I alleles, where a multi-epitope vaccine would cover a larger percentage of the population than individual epitopes could.

3.6. Linear B-cell epitope prediction

In the current study, linear B-cell epitopes were identified by utilizing an amino acid-based method.

The BepiPred linear epitope prediction tool was applied, which is regarded as the best method for predicting linear B-cell epitopes. This tool uses a hidden Markov model. A total of 68 linear epitopes were predicted by BepiPred. By selecting only those with lengths $\geq$7 amino acid residues, 19 epitopes were finally included for further analysis (Table 5). The β-turns were predicted by the Chaus and Fasman β-turn prediction method. Previous research has shown that the antigenic part of the protein mostly remains as β-sheet [78]. The region containing residues 807–813 was predicted to be a β-turn region, with a score of 1.413; this was almost the highest score (Table S5). The region of residues 499–505 had a score of 1.257, and the 1140–1146 region had a score of 1.057; these were all greater than the average score (Fig. 5).

The Emini surface accessibility prediction method was also employed in this study. The average surface accessibility was 1.0, with a minimum of 0.042. In accordance with the above B-cell epitope results, the peptide region of 810–815 was predicted to have the best surface accessibility, with a score of 5.662 (Fig. 5).

The Kolaskar and Tongaonkar method was employed to predict antigenicity. This method evaluates antigenicity based on the physicochemical properties of amino acids and their abundances in experimentally known epitopes. A total of 46 B-cell epitopes were predicted by this method (Table 6). The average antigenic propensity of the SARS-CoV-2 SGP epitopes was 1.041, with a maximum of 1.261. The highest score was found for amino acids 5–11. The regions of 490–496 and 491–497 had equal scores of 1.067 (Fig. 6). The scores for the amino acid regions 558–564, 703–709, and 1140–1146 were 1.065, 1.026, and 1.051, respectively, and were all greater than the average value (Fig. 6).

The Karplus and Schulz flexibility prediction method found an average flexibility of 0.993 and a minimum of 0.866. The residue region 809–815 was found to be flexible, with a score of 1.101; this result was nearly the highest score (1.125). The next highest score was for residues

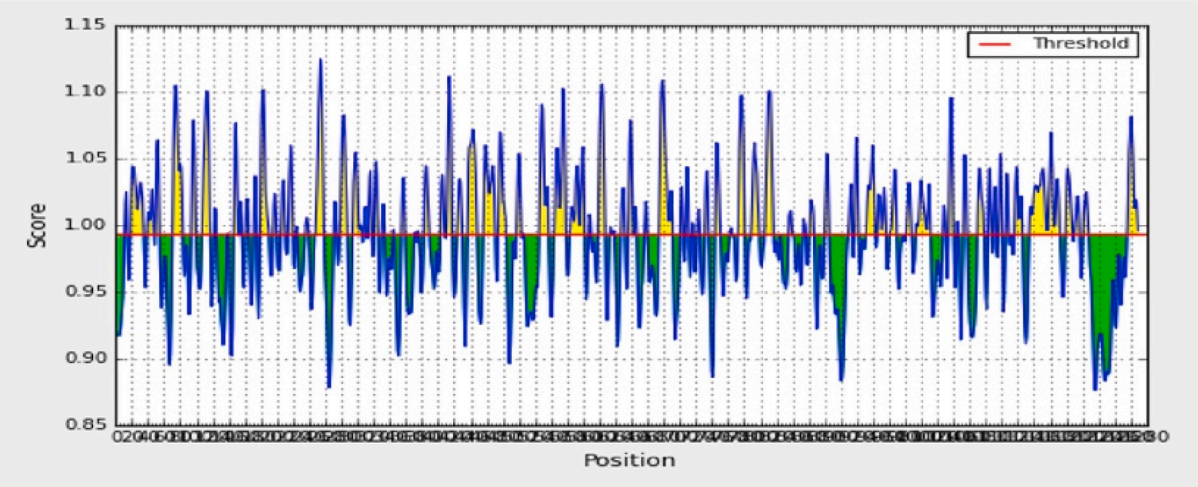

(D)

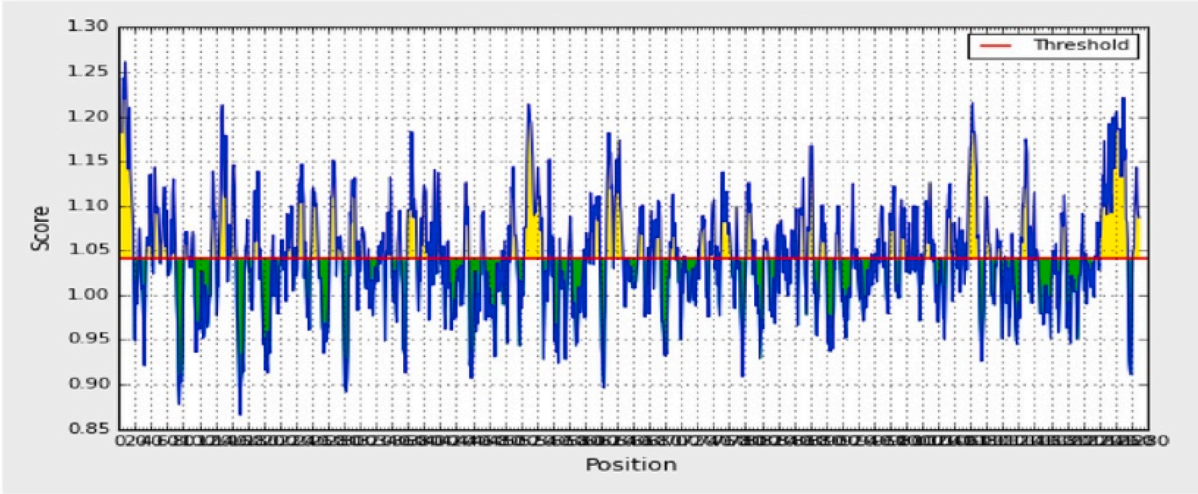

(E)

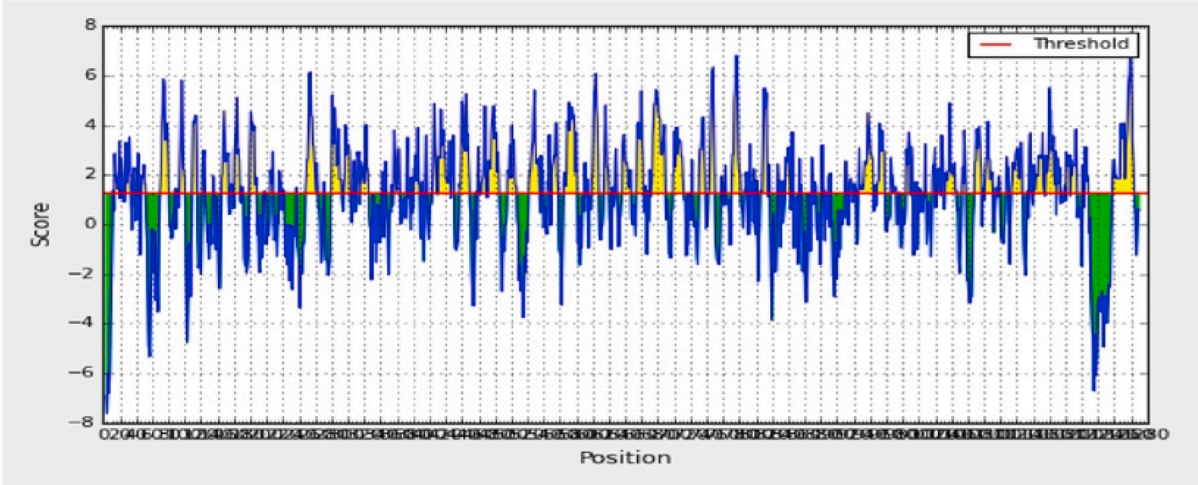

(F)

Fig. 6. Combined B-cell linear epitope prediction using **(D)** Karplus & Schulz flexibility prediction, **(E)** Kolaskar & Tongaonkar antigenicity, **(F)** Parker hydrophilicity prediction methods.

810–816, with a score of 1.1 (Fig. 6). The amino acid regions from 700 to 706, 910–916, and 1140–1146 had very similar scores of 1.029, 1.031, and 1.028, respectively (Fig. 6).

The Parker hydrophilicity prediction tool found an average hydrophilicity score of 1.238 for the SARS-CoV-2 SGP. The highest score was for the amino acid region 1257–1263 (Fig. 6).

Many vaccines are comprised of attenuated or killed pathogens. However, peptide vaccines that are capable of eliciting immune responses against specific pathogens contain peptides that are linear B cell epitopes [79]. The B-cell epitopes are antigenic determinants and are specifically recognized by the immune system because they represent specific pieces of antigens that bind to B lymphocytes; these epitopes are crucial for vaccine design [80]. A previous study demonstrated that linear B-cell epitopes can induce immunity against *Pseudomonas aeruginosa* in mice [81]. Synthetic peptides that contain linear B-cell epitopes are pivotal for producing antibodies against a specific protein; these antibodies can be used in various applications, such as in diagnostic tools or screening assays [82]. Importantly, B-cell epitopes elicit strong immune responses and do not cause any side effects. Here, we also predicted B-cell epitopes utilizing the IEDB database. The recent study by Grifoni et al. predicted B-cell epitopes of SARS-CoV-2 and SARS-CoV; the authors found that the SGP of SARS-CoV-2 contained the largest number of B-cell epitopes [77]. Moreover, they also predicted seven epitope regions of the SARS-CoV-2 SGP, which were the amino acid residues 491–505, 558–562, 703–704, 793–794, 810, 914, and 1140–1146. In the current study, we utilized several tools from the IEDB database to predict linear B-cell epitopes. As a result, we identified several B-cell epitopes from the SARS-CoV-2 SGP that are in agreement with those identified by Grifoni et al. (Table S6) [77]. In addition, the Grifoni study found that the predicted epitopes had a sequence identity greater than 65% [77]. The predicted B-cell epitopes were also in agreement with another previous study that had predicted several SARS-CoV-2 SGP B-cell epitopes (Table S6) [83].

Our study is not exhaustive, and *in silico* work has several pros and cons. The vaccine development process is tedious, and it can take years to develop a vaccine for use in humans, especially when the technologies are new and have not been extensively used before. Although institutes such as Curevac, Inovio, and Applied DNA Sciences are working on vaccines focusing on the SGP of SARS-CoV-2, it is not possible to predict how long it will take to obtain a successful vaccine. Realistically, an animal model is a prerequisite for testing the protectiveness of a vaccine, but developing an animal model for SARS-CoV-2 has been difficult. Vaccines also must be tested for toxicity in various animals, for example, rabbits, which typically takes several months to complete. Human vaccines must be produced in accordance with current good manufacturing practices (cGMPs), which requires trained personnel, exclusive facilities, appropriate documentation, and quality raw materials. As a result, vaccine candidates that are in the preclinical phase might require specialized processes that need to be developed from scratch. Realistically, it will require more than 1 year to license any vaccine for SARS-CoV-2.

4. Conclusions

Improvements in the field of immunoinformatics have been an important factor in advancing the prediction of peptide-based vaccines. Viruses can activate both T-cell and humoral immunity. The epitopes predicted in this study might improve immunity against SARS-CoV-2. Our work is based on the fundamental principles of immunity, whereby the recognition of foreign bodies by the host immune cells provokes an immune response in which relevant information is transferred to both T cells and B cells. Here, utilizing *in silico* simulations, our predicted epitopes were able to interact with $CD8^{+}$ cells when the epitopes were presented as antigens. However, the present study is only a preliminary approach for predicting an epitope-based vaccine against SARS-CoV-2. We hope that these predicted epitopes will lay the foundation for the further experimental design of vaccine candidates against SARS-CoV-2.

Declaration of competing interest

The author declares that there is no competing interest in this work.

Acknowledgments

The authors would like to thank Cambridge Proofreading & Editing LLC. (https://proofreading.org/) for editing a draft of this manuscript. Prof. T. Ben Hadda acknowledges the offer of the bioinformatics facilities by Prof Y. Zarhloule even in this critical situation of COVID-19, and the financially support by the Deanship of Scientific Research at Umm Al-Qura University to Prof. F.A. Almalki (18-MED-1-02-0003).

Appendix A. Supplementary data

Supplementary data related to this article can be found at https://doi.org/10.1016/j.compbiomed.2020.103967.

Data availability

The raw data supporting the conclusions of this manuscript will be made available by the authors, without undue reservation, to any qualified researcher.

Author contributions

Study concept and design: A.R., S.A.S., T.B.H., F.A.A., and T.B.E. Acquisition of data: A.R., S.A.S., A.S., A.P. F.A.A. and T.B.H. Analyses and interpretation of data: A.R., S.A.S., A.M.T., N.U.E., N.J.M., M.M.C., T.A.E., S.C., S.S., F.N. and T.B.E. Drafting the manuscript: A.R., S.A.S., S. J.M., F.A.A., T.B.H., and T.B.E. Critical revision of the manuscript for important intellectual content: S.J.M., F.A.A., T.B.H., and T.B.E. Technical or material support: A.R. Study supervision: F.A.A., T.B.H., and T. B.E.

Funding

This work is conducted with the individual funding of all authors.

Ethical approval

Not required.

ORCID identification

- A. Rakib: https://orcid.org/0000-0003-3335-0368
- F. Nainu: https://orcid.org/0000-0003-0989-4023
- A. Paul: https://orcid.org/0000-0002-2767-2646
- A. Shahriar: https://orcid.org/0000-0001-5529-8893
- A.M. Tareq: https://orcid.org/0000-0003-2704-7610
- N.U. Emon: https://orcid.org/0000-0001-7567-4796
- S. Chakraborty: https://orcid.org/0000-0002-0178-4869
- T. Ben Hadda: https://orcid.org/0000-0002-5633-6203.
- F.A. Almalki: https://orcid.org/0000-0003-4048-1526
- T. Bin Emran: https://orcid.org/0000-0003-3188-2272

References

[1] D. Wang, B. Hu, C. Hu, F. Zhu, X. Liu, J. Zhang, B. Wang, H. Xiang, Z. Cheng, Y. Xiong, et al., Clinical characteristics of 138 hospitalized patients with 2019 novel coronavirus–infected pneumonia in Wuhan, China, JAMA 323 (3) (2020) 1061–1069.

[2] Q. Li, X. Guan, P. Wu, X. Wang, L. Zhou, Y. Tong, R. Ren, K.S.M. Leung, E.H.Y. Lau, J.Y. Wong, et al., Early transmission dynamics in Wuhan, China, of novel coronavirus–infected pneumonia, N. Engl. J. Med. 382 (13) (2020) 1199–1207.

[3] L.E. Gralinski, V.D. Menachery, Return of the coronavirus: 2019-nCoV, Viruses 12 (2020) 135.

[4] W.H. Organization, et al., Coronavirus Disease 2019 (COVID-19): Situation Report, vol. 72, 2020.

[5] D.A.J. Tyrrell, M.L. Bynoe, et al., Cultivation of viruses from a high proportion of patients with colds, Lancet (1966) 76–77.

[6] J.M. Christie, H. Chapel, R.W. Chapman, W.M. Rosenberg, Immune selection and genetic sequence variation in core and envelope regions of hepatitis C virus, Hepatology 30 (1999) 1037–1044.

[7] D. Yang, J.L. Leibowitz, The structure and functions of coronavirus genomic 3′ and 5′ ends, Virus Res. 206 (2015) 120–133.

[8] C. Xiong, L. Jiang, Y. Chen, Q. Jiang, Evolution and Variation of 2019-novel Coronavirus, Biorxiv, 2020.

[9] P. Zhou, X.-L. Yang, X.-G. Wang, B. Hu, L. Zhang, W. Zhang, H.-R. Si, Y. Zhu, B. Li, C.-L. Huang, et al., A pneumonia outbreak associated with a new coronavirus of probable bat origin, Nature 579 (2020) 270–273.

[10] J.P. Kanne, Chest CT Findings in 2019 Novel Coronavirus (2019-nCoV) Infections from Wuhan, China: Key Points for the Radiologist, 2020.

[11] S. Sanche, Y.T. Lin, C. Xu, E. Romero-Severson, N. Hengartner, R. Ke, Early Release-High Contagiousness and Rapid Spread of Severe Acute Respiratory Syndrome Coronavirus vol. 2, (n.d.).

[12] W.H. Organization, et al., Q&A on Coronaviruses (COVID-19), Retrieved April 6th. (2020).

[13] W.H. Organization, et al., Modes of transmission of virus causing COVID-19: implications for IPC precaution recommendations: scientific brief, 29 March 2020, p. 2020.

[14] N. Chen, M. Zhou, X. Dong, J. Qu, F. Gong, Y. Han, Y. Qiu, J. Wang, Y. Liu, Y. Wei, et al., Epidemiological and clinical characteristics of 99 cases of 2019 novel coronavirus pneumonia in Wuhan, China: a descriptive study, Lancet 395 (2020) 507–513.

[15] M.L. Holshue, C. DeBolt, S. Lindquist, K.H. Lofy, J. Wiesman, H. Bruce, C. Spitters, K. Ericson, S. Wilkerson, A. Tural, et al., First case of 2019 novel coronavirus in the United States, N. Engl. J. Med. 382 (10) (2020) 929–936.

[16] S.F. Ahmed, A.A. Quadeer, M.R. McKay, Preliminary Identification of Potential Vaccine Targets for the COVID-19 Coronavirus (SARS-CoV-2) Based on SARS-CoV Immunological Studies, 2020, https://doi.org/10.3390/v12030254. Viruses.

[17] F. Wu, S. Zhao, B. Yu, Y.-M. Chen, W. Wang, Y. Hu, Z.-G. Song, Z.-W. Tao, J.-H. Tian, Y.-Y. Pei, et al., Complete Genome Characterisation of a Novel Coronavirus Associated with Severe Human Respiratory Disease in Wuhan, BioRxiv, China, 2020.

[18] A.C. Walls, Y.-J. Park, M.A. Tortorici, A. Wall, A.T. McGuire, D. Veesler, Structure, function, and antigenicity of the SARS-CoV-2 spike glycoprotein, Cell 181 (2) (2020) 281–292.

[19] M.A. Tortorici, D. Veesler, Structural insights into coronavirus entry, Adv. Virus Res. 105 (2019) 93–116.

[20] X. Zhu, Q. Liu, L. Du, L. Lu, S. Jiang, Receptor-binding domain as a target for developing SARS vaccines, J. Thorac. Dis. 5 (2013) S142.

[21] D.L. Suarez, S. Schultz-Cherry, Immunology of avian influenza virus: a review, Dev. Comp. Immunol. 24 (2000) 269–283.

[22] B. Briney, D. Sok, J.G. Jardine, D.W. Kulp, P. Skog, S. Menis, R. Jacak, O. Kalyuzhniy, N. De Val, F. Sesterhenn, et al., Tailored immunogens direct affinity maturation toward HIV neutralizing antibodies, Cell 166 (2016) 1459–1470.

[23] D.S. Rosa, S.P. Ribeiro, E. Cunha-Neto, CD4+ T cell epitope discovery and rational vaccine design, Arch. Immunol. Ther. Exp. (Warsz). 58 (2010) 121–130.

[24] J. Liu, S. Zhang, S. Tan, B. Zheng, G.F. Gao, Revival of the identification of cytotoxic T-lymphocyte epitopes for immunological diagnosis, therapy and vaccine development, Exp. Biol. Med. 236 (2011) 253–267.

[25] B. Cao, Y. Wang, D. Wen, W. Liu, J. Wang, G. Fan, L. Ruan, B. Song, Y. Cai, M. Wei, et al., A trial of lopinavir–ritonavir in adults hospitalized with severe Covid-19, N. Engl. J. Med. 382 (19) (2020) 1787–1799.

[26] Q. Gao, L. Bao, H. Mao, L. Wang, K. Xu, M. Yang, Y. Li, L. Zhu, N. Wang, Z. Lv, et al., development of an inactivated vaccine candidate for SARS-CoV-2, Science (2020) (80–.).

[27] H. Wang, Y. Zhang, B. Huang, W. Deng, Y. Quan, W. Wang, W. Xu, Y. Zhao, N. Li, J. Zhang, et al., Development of an Inactivated Vaccine Candidate, BBIBP-CorV, with Potent Protection against SARS-CoV-2, Cell, 2020.

[28] J. Zhang, H. Zeng, J. Gu, H. Li, L. Zheng, Q. Zou, Progress and prospects on vaccine development against SARS-CoV-2, Vaccines 8 (2020) 153.

[29] G.A. Poland, I.G. Ovsyannikova, R.B. Kennedy, I.H. Haralambieva, R.M. Jacobson, Vaccinomics and a new paradigm for the development of preventive vaccines against viral infections, OMICS A J. Integr. Biol. 15 (2011) 625–636.

[30] A. Rakib, S.A. Sami, M.A. Islam, S. Ahmed, F.B. Faiz, B.H. Khanam, K.K.S. Marma, M. Rahman, M.M.N. Uddin, T. Bin Emran, et al., Epitope-Based Immunoinformatics Approach on Nucleocapsid Protein of Severe Acute Respiratory Syndrome-Coronavirus-2, 2020.

[31] K.A. Peele, T. Srihansa, S. Krupanidhi, A.V. Sai, T.C. Venkateswarulu, Design of multi-epitope vaccine candidate against SARS-CoV-2: a in-silico study, J. Biomol. Struct. Dyn. (2020) 1.

[32] E. Ong, M.U. Wong, A. Huffman, Y. He, COVID-19 Coronavirus Vaccine Design Using Reverse Vaccinology and Machine Learning, BioRxiv, 2020.

[33] C.H. Lee, H. Koohy, In Silico Identification of Vaccine Targets for 2019-nCoV, 2020. F1000Research. 9.

[34] L. Du, G. Zhao, L. Li, Y. He, Y. Zhou, B.-J. Zheng, S. Jiang, Antigenicity and immunogenicity of SARS-CoV S protein receptor-binding domain stably expressed in CHO cells, Biochem. Biophys. Res. Commun. 384 (2009) 486–490.

[35] UniProt, The universal protein knowledgebase, Nucleic Acids Res. 45 (2017) D158–D169.

[36] W. Li, A. Cowley, M. Uludag, T. Gur, H. McWilliam, S. Squizzato, Y.M. Park, N. Buso, R. Lopez, The EMBL-EBI bioinformatics web and programmatic tools framework, Nucleic Acids Res. 43 (2015) W580–W584.

[37] I.A. Doytchinova, D.R. Flower, VaxiJen: a server for prediction of protective antigens, tumour antigens and subunit vaccines, BMC Bioinf. 8 (2007) 4.

[38] D.L. Bugembe, A.O. Ekii, N. Ndembi, J. Serwanga, P. Kaleebu, P. Pala, Computational MHC-I epitope predictor identifies 95% of experimentally mapped HIV-1 clade A and D epitopes in a Ugandan cohort, BMC Infect. Dis. 20 (2020) 1–16.

[39] R. Vita, S. Mahajan, J.A. Overton, S.K. Dhanda, S. Martini, J.R. Cantrell, D. K. Wheeler, A. Sette, B. Peters, The immune epitope database (IEDB): 2018 update, Nucleic Acids Res. 47 (2019) D339–D343.

[40] S. Giguère, A. Drouin, A. Lacoste, M. Marchand, J. Corbeil, F. Laviolette, MHC-NP: predicting peptides naturally processed by the MHC, J. Immunol. Methods 400 (2013) 30–36.

[41] H.-H. Bui, J. Sidney, W. Li, N. Fusseder, A. Sette, Development of an epitope conservancy analysis tool to facilitate the design of epitope-based diagnostics and vaccines, BMC Bioinf. 8 (2007) 361.

[42] M. Moutaftsi, B. Peters, V. Pasquetto, D.C. Tscharke, J. Sidney, H.-H. Bui, H. Grey, A. Sette, A consensus epitope prediction approach identifies the breadth of murine T CD8+-cell responses to vaccinia virus, Nat. Biotechnol. 24 (2006) 817–819.

[43] I. Dimitrov, D.R. Flower, I. Doytchinova, AllerTOP-a server for in silico prediction of allergens, BMC Bioinf. (2013) S4.

[44] J. Maupetit, P. Derreumaux, P. Tuffery, PEP-FOLD: an online resource for de novo peptide structure prediction, Nucleic Acids Res. 37 (2009) W498–W503.

[45] N. Guex, M.C. Peitsch, SWISS-MODEL and the Swiss-Pdb Viewer: an environment for comparative protein modeling, Electrophoresis 18 (1997) 2714–2723.

[46] S. Dallakyan, PyRx-python Prescription V. 0.8, Scripps Res. Inst, 2008, p. 2010.

[47] N.M. O'Boyle, M. Banck, C.A. James, C. Morley, T. Vandermeersch, G. R. Hutchison, Open Babel: an open chemical toolbox, J. Cheminf. 3 (2011) 33.

[48] O. Trott, A.J. Olson, AutoDock Vina, Improving the speed and accuracy of docking with a new scoring function, efficient optimization, and multithreading, J. Comput. Chem. (2009), https://doi.org/10.1002/jcc.21334.

[49] M. Nielsen, C. Lundegaard, P. Worning, S.L. Lauemøller, K. Lamberth, S. Buus, S. Brunak, O. Lund, Reliable prediction of T-cell epitopes using neural networks with novel sequence representations, Protein Sci. 12 (2003) 1007–1017.

[50] J. Greenbaum, J. Sidney, J. Chung, C. Brander, B. Peters, A. Sette, Functional classification of class II human leukocyte antigen (HLA) molecules reveals seven different supertypes and a surprising degree of repertoire sharing across supertypes, Immunogenetics 63 (2011) 325–335.

[51] H.-H. Bui, J. Sidney, K. Dinh, S. Southwood, M.J. Newman, A. Sette, Predicting population coverage of T-cell epitope-based diagnostics and vaccines, BMC Bioinf. 7 (2006) 1–5.

[52] E.A. Emini, J. V Hughes, D. Perlow, J. Boger, Induction of hepatitis A virus-neutralizing antibody by a virus-specific synthetic peptide, J. Virol. 55 (1985) 836–839.

[53] A.S. Kolaskar, P.C. Tongaonkar, A semi-empirical method for prediction of antigenic determinants on protein antigens, FEBS Lett. 276 (1990) 172–174.

[54] P.A. Karplus, G.E. Schulz, Prediction of chain flexibility in proteins, Naturwissenschaften 72 (1985) 212–213.

[55] J.E.P. Larsen, O. Lund, M. Nielsen, Improved method for predicting linear B-cell epitopes, Immunome Res. 2 (2006) 2.

[56] P.Y. Chou, G.D. Fasman, Empirical predictions of protein conformation, Annu. Rev. Biochem. 47 (1978) 251–276.

[57] S.K. Patel, M. Pathak, R. Tiwari, M.I. Yatoo, Y.S. Malik, R. Sah, A.A. Rabaan, K. Sharun, K. Dhama, D.K. Bonilla-Aldana, et al., A Vaccine Is Not Too Far for COVID-19, (n.d.).

[58] A. Ramaiah, V. Arumugaswami, Insights into Cross-Species Evolution of Novel Human Coronavirus 2019-nCoV and Defining Immune Determinants for Vaccine Development, BioRxiv, 2020.

[59] Y. He, Y. Zhou, S. Liu, Z. Kou, W. Li, M. Farzan, S. Jiang, Receptor-binding domain of SARS-CoV spike protein induces highly potent neutralizing antibodies: implication for developing subunit vaccine, Biochem. Biophys. Res. Commun. 324 (2004) 773–781.

[60] L. Du, Z. Kou, C. Ma, X. Tao, L. Wang, G. Zhao, Y. Chen, F. Yu, C.-T.K. Tseng, Y. Zhou, et al., A truncated receptor-binding domain of MERS-CoV spike protein potently inhibits MERS-CoV infection and induces strong neutralizing antibody responses: implication for developing therapeutics and vaccines, PloS One 8 (2013).

[61] M.I. Abdelmageed, A.H. Abdelmoneim, M.I. Mustafa, N.M. Elfadol, N.S. Murshed, S.W. Shantier, A.M. Makhawi, Design of a multiepitope-based peptide vaccine against the E protein of human COVID-19: an immunoinformatics approach, BioMed Res. Int. 2020 (2020).

[62] M. Dalsass, A. Brozzi, D. Medini, R. Rappuoli, Comparison of open-source reverse vaccinology programs for bacterial vaccine antigen discovery, Front. Immunol. 10 (2019) 113.

[63] J.T. Ortega, M.L. Serrano, F.H. Pujol, H.R. Rangel, Role of changes in SARS-CoV-2 spike protein in the interaction with the human ACE2 receptor: an in silico analysis, EXCLI J. 19 (2020) 410.

[64] S.K. Sinha, A. Shakya, S.K. Prasad, S. Singh, N.S. Gurav, R.S. Prasad, S.S. Gurav, An in-silico evaluation of different Saikosaponins for their potency against SARS-CoV-

2 using NSP15 and fusion spike glycoprotein as targets, J. Biomol. Struct. Dyn. (2020) 1–12.
[65] D.C. Chan, D. Fass, J.M. Berger, P.S. Kim, Core structure of gp41 from the HIV envelope glycoprotein, Cell 89 (1997) 263–273.
[66] W. Weissenhorn, A. Dessen, S.C. Harrison, J.J. Skehel, D.C. Wiley, Atomic structure of the ectodomain from HIV-1 gp41, Nature 387 (1997) 426–430.
[67] T. Kallinich, K.C. Beier, U. Wahn, P. Stock, E. Hamelmann, T-cell co-stimulatory molecules: their role in allergic immune reactions, Eur. Respir. J. 29 (2007) 1246–1255.
[68] B. Alberts, A. Johnson, J. Lewis, M. Raff, K. Roberts, P. Peter Walter, Molecular Biology of the Cell, Garland Science.[Google Scholar], New York, 2002.
[69] S. Ahmed, A. Rakib, M.A. Islam, B.H. Khanam, F.B. Faiz, A. Paul, M.N.U. Chy, N.M. M.A. Bhuiya, M.M.N. Uddin, S.M.A. Ullah, et al., In vivo and in vitro pharmacological activities of *Tacca integrifolia* rhizome and investigation of possible lead compounds against breast cancer through in silico approaches, Clin. Phytosci. 5 (2019) 36.
[70] A. Khanolkar, V.P. Badovinac, J.T. Harty, CD8 T cell memory development: CD4 T cell help is appreciated, Immunol. Res. 39 (2007) 94–104.
[71] M.J. Bevan, Helping the CD8+ T-cell response, Nat. Rev. Immunol. 4 (2004) 595–602.
[72] P. Novy, M. Quigley, X. Huang, Y. Yang, CD4 T cells are required for CD8 T cell survival during both primary and memory recall responses, J. Immunol. 179 (2007) 8243–8251.
[73] S.-S. Chiou, Y.-C. Fan, W.D. Crill, R.-Y. Chang, G.-J.J. Chang, Mutation analysis of the cross-reactive epitopes of Japanese encephalitis virus envelope glycoprotein, J. Gen. Virol. 93 (2012) 1185–1192.
[74] P. Oyarzún, J.J. Ellis, M. Bodén, B. Kobe, PREDIVAC: CD4+ T-cell epitope prediction for vaccine design that covers 95% of HLA class II DR protein diversity, BMC Bioinf. 14 (2013) 1–11.
[75] M.K. Khan, S. Zaman, S. Chakraborty, R. Chakravorty, M.M. Alam, T.R. Bhuiyan, M.J. Rahman, C. Fernández, F. Qadri, Z.I. Seraj, In silico predicted mycobacterial epitope elicits in vitro T-cell responses, Mol. Immunol. 61 (2014) 16–22.
[76] A. Alam, S. Ali, S. Ahamad, M.Z. Malik, R. Ishrat, From ZikV genome to vaccine: in silico approach for the epitope-based peptide vaccine against Zika virus envelope glycoprotein, Immunology 149 (2016) 386–399.
[77] A. Grifoni, J. Sidney, Y. Zhang, R.H. Scheuermann, B. Peters, A. Sette, A Sequence Homology and Bioinformatic Approach Can Predict Candidate Targets for Immune Responses to SARS-CoV-2, Cell Host Microbe, 2020.
[78] A. Hasan, M. Hossain, J. Alam, A computational assay to design an epitope-based Peptide vaccine against Saint Louis encephalitis virus, Bioinf. Biol. Insights 7 (2013). BBI–S13402.
[79] E.H. Nardin, J.M. Calvo-Calle, G.A. Oliveira, R.S. Nussenzweig, M. Schneider, J.-M. Tiercy, L. Loutan, D. Hochstrasser, K. Rose, A totally synthetic polyoxime malaria vaccine containing Plasmodium falciparum B cell and universal T cell epitopes elicits immune responses in volunteers of diverse HLA types, J. Immunol. 166 (2001) 481–489.
[80] R.A. Shey, S.M. Ghogomu, K.K. Esoh, N.D. Nebangwa, C.M. Shintouo, N. F. Nongley, B.F. Asa, F.N. Ngale, L. Vanhamme, J. Souopgui, In-silico design of a multi-epitope vaccine candidate against onchocerciasis and related filarial diseases, Sci. Rep. 9 (2019) 1–18.
[81] E.E. Hughes, H.E. Gilleland Jr., Ability of synthetic peptides representing epitopes of outer membrane protein F of Pseudomonas aeruginosa to afford protection against P. aeruginosa infection in a murine acute pneumonia model, Vaccine 13 (1995) 1750–1753.
[82] G.A. Schellekens, H. Visser, B.A.W. De Jong, F.H.J. Van Den Hoogen, J.M. W. Hazes, F.C. Breedveld, W.J. Van Venrooij, The diagnostic properties of rheumatoid arthritis antibodies recognizing a cyclic citrullinated peptide, Arthritis Rheum. Off. J. Am. Coll. Rheumatol. 43 (2000) 155–163.
[83] M. Bhattacharya, A.R. Sharma, P. Patra, P. Ghosh, G. Sharma, B.C. Patra, S.-S. Lee, C. Chakraborty, Development of epitope-based peptide vaccine against novel coronavirus 2019 (SARS-COV-2): immunoinformatics approach, J. Med. Virol. 92 (2020) 618–631.